Reabsorption losses in Luminescent Solar Concentrators

Sara Peeters

Promotoren: prof. dr. ir. Kristiaan Neyts, Dick de Boer (Philips)
Begeleiders: Pieter Vanbrabant, prof. Jeroen Beeckman

Masterproef ingediend tot het behalen van de academische graad van
Master in de ingenieurswetenschappen: fotonica

Vakgroep Elektronica en Informatiesystemen
Voorzitter: prof. dr. ir. Jan Van Campenhout
Faculteit Ingenieurswetenschappen en Architectuur
Academiejaar 2010-2011

UNIVERSITEIT
GENT

Reabsorption losses in Luminescent Solar Concentrators

Sara Peeters

Promotoren: prof. dr. ir. Kristiaan Neyts, Dick de Boer (Philips)
Begeleiders: Pieter Vanbrabant, prof. Jeroen Beeckman

Masterproef ingediend tot het behalen van de academische graad van
Master in de ingenieurswetenschappen: fotonica

Vakgroep Elektronica en Informatiesystemen
Voorzitter: prof. dr. ir. Jan Van Campenhout
Faculteit Ingenieurswetenschappen en Architectuur
Academiejaar 2010-2011

UNIVERSITEIT
GENT

Preface

Luminescent solar concentrators is one of those research subjects that are not very well known to the general public. For this reason I also first heard about it just over a year ago. From the beginning, it appeared to me as a meaningful way of trying to accomplish something in renewable energy and solar cell research. Altough the impact I could make during the one year I was working on this master thesis was small, at least I have explained to many people in my surroundings that there exists something like a luminescent solar concentrator. Moreover, the impact this year has made on me should certainly not be called small. Having been able to work at Philps Research in Eindhoven as an intern during 5 months, and working on this master thesis in general, was a valuable learning experience, and I am grateful to whoever made this possible.

I would like to thank my supervisors: Kristiaan Neyts, Dick de Boer, Pieter Vanbrabant and Jeroen Beeckman, for their help during this year. Also thanks to Shufen Tsoi and Michael Debye from TU/e and to Hugo Cornelissen from Philips, who were always there when I wanted to discuss my results, or needed specific tools for the experiments. Also to all other people form Ghent University, TU Eindhoven or Philips, who helped me with smaller or larger problems,patiently explained me things I didn't know, or simply made me feel at ease, thanks a lot for that.

Special thanks goes to my boyfriend Steven, for always being there for me, even when physically far away, and to my parents, who have always believed in me and suported me, and without whom I would not be where I am now.

Sara Peeters
Gent, mei 2011

Toelating tot bruikleen
Permission of use

Reabsorption losses in Luminescent Solar Concentrators

door

Sara Peeters

Masterproef ingediend tot het behalen van de academische graad van

Master in de ingenieurswetenschappen: fotonica

Academiejaar 2010–2011

Promotoren: Prof. Dr. Ir. K. Neyts, D. de Boer(Philips)

Begeleider: P. Vanbrabant, prof. J. Beeckman

Faculteit Ingenieurswetenschappen en architectuur

Universiteit Gent

Vakgroep Elektronica en Informatiesystemen

Voorzitter: Prof. Dr. Ir. J. Van Campenhout

Samenvatting

Met de ontwikkeling van *luminescent solar concentrators* probeert men zonlicht op een slimme manier te concentreren op een kleinere fotovoltaische zonnecel. Zo kan men niet alleen een groter deel van het zonnespectrum gebruiken, maar ook op een goedkopere manier electriciteit uit zonlicht winnen. Het minimaliseren van de verliezen door het gebruik van nieuwe materialen en filters is een cruciale stap in dit ontwikkelingsproces.

In dit werk worden reabsorptieverliezen in *luminescent solar concentrators* onderzocht door middel van experimenten en simulaties. Door samples op verschillende afstanden van het uiteinde te belichten met een geschikte LED-bron, kunnen reabsorptieverliezen gemakkelijk gekarakterizeerd worden. Voor de simulatie van de experimentele situatie met raytracing software zoals het hier gebruikte programma LightTools is kennis van de eigenschapen van de zijwanden van het sample noodzakelijk. De vergelijking tussen de gemeten en gesimuleerde spectra kan dan uitsluitsel geven over de al dan niet correcte implementatie van reabsorptieverliezin in het simulatieprogramma.

Trefwoorden

Luminescent solar concentrator, reabsorptieverliezen, Lumogen F Rot 305, collectie-efficientie, reabsorptiewaarschijnlijkheid, LightTools

Reabsorption losses in Luminescent Solar Concentrators

Sara Peeters

Supervisors: Kristiaan Neyts, Dick de Boer, Pieter Vanbrabant, Jeroen Beeckman

Abstract— **In this article, reabsorption losses in luminescent solar concentrators (LSCs) are investigated both through experiments and computer simulations. Lumogen F Rot 305, coated on top of a PMMA plate is used as a dye. The aim is to better understand reabsorption losses and to be able to implement them correctly in ray-tracing simulations. To this purpose, the edge emission of a locally illuminated sample is measured. The experimental situation is also modeled in LightTools and the results are compared.**

Keywords— **Luminescent solar concentrator, reabsorption losses, Lumogen F Rot 305, collection efficiency, reabsorption probability, LightTools**

I. Introduction

LUMINESCENT SOLAR CONCENTRATORS use organic or inorganic luminescent materials embedded in or coated on top of a slab of transparent material (e.g. glass, PMMA) to concentrate light. The incoming sunlight is absorbed by the dyes in the slab, and reemitted at a longer wavelength and in a random direction. Next, most of the luminescent light is guided towards the edges of the slab by total internal reflection. At one or more edges, photovoltaic cells are attached. They convert the incident light into electricity. Because of the concentration of the light in the slab, less photovoltaic cell area is needed to obtain the same amount of electricity.

LSCs were first investigated in the seventies [1]. However, interest soon diminished as the quality of the luminescent materials at the time was not suficient. Thanks to the discovery of new materials and the growing importance of cheap renewable energy resources, luminescent solar concentrators have again become an important research topic today.

Most research attention goes to the development of luminescent materials [2] and filters [3] in order to reduce the losses and make the LSC economicaly viable.

Reabsorption is an important loss factor caused by the overlap between the absorption and the emission spectrum of the used dye. Luminescent photons emitted in this overlap region, risk to be absorbed again by another dye molecule and get lost instead of reaching the edge of the concentrator. This important loss mechanism will be investigated using experiments and computer simulations.

II. Experiment

A. Set-up

In the experiments $50 \times 50 \times 5$ mm samples were measured. One of the small edges was painted black and the luminescent output of the opposite edge was measured. This edge will further be referred to as the measurement edge. The sample was sitting on a black table, with the measurement edge facing a 50×5 mm rectangular hole in an integrating sphere. To this integrating sphere, a completely calibrated spectrometer (Labsphere) was attached. The sample was covered with dark cardboard, exept for a 50×5 mm line at a certain distance of the measurement edge. Here the sample was illuminated using a blue or a green LED. Those were chosen in particular for use with the lumogen red dye because they correspond to peaks in the absorption spectrum and do not overlap with the emission spectrum. So the transmitted LED light can be easily separated from the luminescent light. A schematic overview of the set-up is given in figure 1. The distance between the illumination line and the measurement edge was varied, and for each distance the luminescent spectrum was registered.

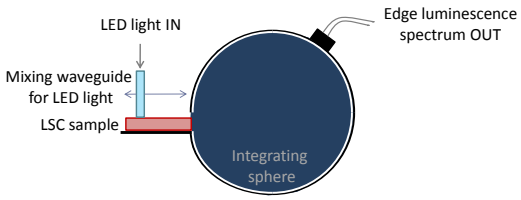

Fig. 1: Measurement setup used for the experiments.

B. Collection efficiency

The collection efficiency (η_{col}) is a quantity incorporating all the losses from the moment a photon is absorbed by a dye molecule for the first time until the light comes out of the measurement edge. It is obtained by dividing the amount of luminescent light coming out of the measurement edge (as a number of photons) by the amount of light that is absorbed by the dye(as a number of photons). One obtains the overall efficiency of te LSC system by multiplying η_{col} with the absorption efficiency (η_{abs}) and the external efficiency of the attached photovoltaic cell (η_{PV}).

In figure 2 the collection efficiency is set out as a function of the illumination distance to the measurement edge. It can be seen that it is independent of the excitation wavelength, and that it decreases with increasing distance. This decrease is due to the loss mechanisms taking place.

C. Reabsorption probability

Where the decrease of the collection efficiency is caused by all kinds of losses, the reabsorption probability(P_r) is a measure specifically for reabsorption losses. It is related to the survival probability(P_0) as $P_0 = 1 - P_r$. The survival probability is defined as the probability that a first time emitted photon reaches the edge of the plate without being reabsorbed.

S. Peeters is currently studying photonics science and engineering at the faculty of engineering and architecture, Ghent University (Belgium). Contact: Sara.Peeters@UGent.be

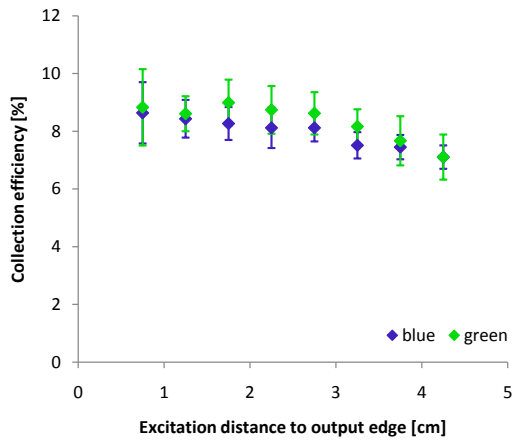

Fig. 2: collection efficiency as a function of excitation distance for blue and green LED light.

The survival probability as a function of excitation distance was plotted in figure 3.

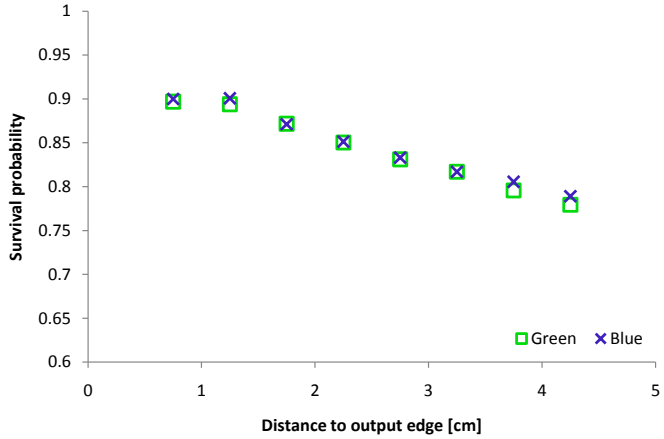

Fig. 3: Reabsorption probability as a function of excitation distance for blue and green LED light.

III. Simulation

A. LightTools, a simulation tool based on raytracing

Raytracing is often used for simulating LSCs. In this case, LightTools was used as a simulation tool, bacause of its ability to simulate luminescent molecules accurately. Except for the exact properties of the edges of the sample(specular reflecting, Lambertian scattering, etc.), all parameters of the experimental situation were known or could be estimated. The influence of the edge properties on the collection efficiency and on the output spectra were than investigated.

B. Collection efficiencies for different edge properties

In figure 4 the simulated collection efficiencies for different edge properties were compared to the experimental situation. It can be seenthat the influence of the edge properties, especially for such small sample sizes as used in our experiments, is rather large. The simulation called complete scattering 3 comes closest to the real situation. In this case the edges were set to be 25% transmissive, and 75% reflective. Both for reflection and transmission, half of the light is scattered and half of it is quasi (cos^5 distribution) specular.

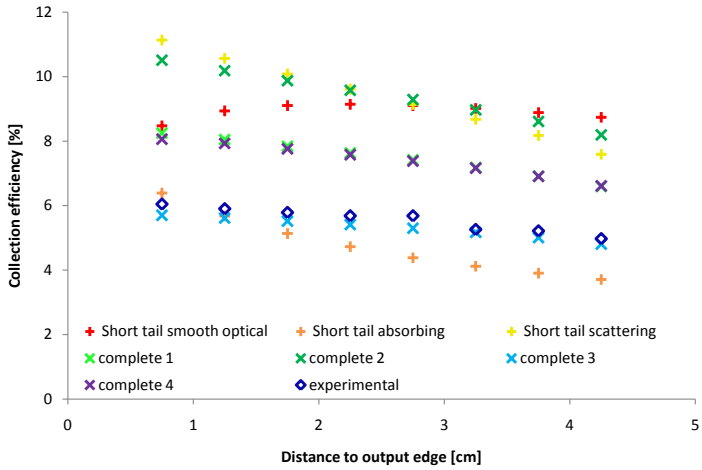

Fig. 4: Simulated and experimental collection efficiencies as a function of excitation distance for the blue LED light.(In this case the energy of the light (Watt) and not the amount of photons is used in nominator and denominator of the collection efficiency)

C. Spectra for different edge properties

The output spectra are found to be strongly dependent on the edge properties. They are in fact the cause of the collection efficiency dependency described above. The edge properties indeed directly influence the pathlength of the light before it reaches the measurement edge. Longer pathlengths give rise to more reabsorption and thus larger reabsorption losses.

In particular we are interested in the red-shift of the spectra indicating the reabsorption of light in the overlap region at the lower wavelength edge of the emission spectrum of the dye. If this red-shift is correctly simulated at larger excitation distances we may believe that the reabsorption in the LSC is properly simulated.

IV. Conclusions

The experimental set-up used, can be further developed to use as an easy tool to characterize and compare reabsorption in LSCs. An extra set-up should be developed to measure the edge properties of the used samples. If such a set-up can be build, the LightTools models can be completed, and the experiment described in this work can serve as a benchmark for the raytracing simulations.

References

[1] A. M. Hermann, *Luminescent solar concentrators, a review*, Solar Energy 29 (1982) 323-329.

[2] B. C. Rowan et al., *Advanced material concepts for luminescent solar concentrators*, IEEE journal of selected topics in quantum electronics 14 (2008) 1312-1322.

[3] M. G. Debye et al. , *Effect on the output of a luminescent solar concentrator on application of organic wavelength-selective mirrors*, Applied Optics 49 (2010) 745-751.

Reabsorptieverliezen in Luminescent Solar Concentrators

Sara Peeters

Begeleiders: Kristiaan Neyts, Dick de Boer, Pieter Vanbrabant, Jeroen Beeckman

Abstract—**In dit artikel worden reabsorptieverliezen in *luminescent solar concentrators* (LSC's) onderzocht met behulp van experimenten en computersimulaties. Lumogen F Rot 305, als een coating op een PMMA-plaat wordt hierbij als luminescent materiaal gebruikt. Het doel is om reabsorptieverliezen beter te begrijpen en ze op een correcte manier te integreren in *ray-tracing* simulaties. Hiervoor is een experiment opgesteld waarin we het geëmiteerde luminescente licht aan de zijkant van een sample dat lokaal belicht wordt met een LED meten.Deze experimentele situatie wordt ook gemodelleerd in LightTools en de resultaten van meting en simulatie worden vergeleken.**

Keywords—***Luminescent solar concentrator*, reabsorptieverliezen, Lumogen F Rot 305, collectie-efficientie, reabsorptiewaarschrijnlijkheid, LightTools**

I. Inleiding

LUMINESCENT SOLAR CONCENTRATORS concentreren licht met behulp van organische of anorganische luminescente materialen die geintegreerd zijn in of gecoat zijn op een plaat van transparant materiaal (vb. glas, PMMA). Het invallende zonlicht wordt door de luminescente materialen geabsorbeerd en opnieuw uitgezonden met een langere golflengte en in een random richting. Hierna wordt het grootste deel van het luminescente licht door totale interne reflectie naar de zijkanten van de plaat geleid.Aan één of meerdere zijkanten worden fotovoltaïsche zonnecellen bevestigd. Deze zetten het invallende licht dan om in elekticiteit. Omdat het licht eerst geconcentreerd wordt in de plaat zijn er minder fotovoltaïsche zonnecellen nodig om eenzelfde hoeveelheid elektriciteit op te wekken.

LSC's Werden voor het eerst onderzocht in de jaren zeventig. Maar de interesse erin verminderde snel toen bleek dat de kwaliteit van de luminescente materialen in die tijd nog onvoldoende was. Dankzij de ontdekking van nieuwe materialen en het groeiende belang van goedkope hernieuwbare energiebronnen zijn *luminescent solar concentrators* vandaag terug een belangrijk onderzoeksonderwerp.

De meeste aandacht van de onderzoekers gaat naar het ontwikkelen van luminescente materialen [2] en filters [3] om de verliezen te verminderen en de LSC zo tot een economisch haalbaar alternatief te maken.

Reabsorptie is een belangrijke verliesfactor, veroorzaakt door de overlap tussen het absorptie- en emissiespectrum van het gebruikte luminescente materiaal. Luminescente fotonen die in dit overlappingsgebied worden uitgezonden, riskeren om opnieuw geabsorbeerd te worden door een andere luminescente molecule en verloren te gaan zonder de zijkant te bereiken. Dit belangrijke verliesmechanisme zal hier onderzocht worden met behulp van experimenten en computersimulaties.

S. Peeters studeert inegenieurswetenschappen: fotonica aan de faculteit ingenieurswetenschappen en architectuur, Universiteit Gent (België). Contact: Sara.Peeters@UGent.be

II. Experiment

A. Opstelling

In de experimenten werden samples van $50 \times 50 \times 5$ mm gebruikt. Eén van de zijkanten was zwart geverfd en de luminescente output van de tegenoverliggende zijkant werd gemeten. We zullen aan deze zijkant refereren als de meetzijde. Het sample lag op een zwarte sample-tafel, met de meetzijde naar 50×5 mm gat in een integrerende sfeer gericht. Aan deze integrerende sfeer was bovendien een volledig gecalibreerde spectrometer (Labsphere) bevestigd. Het sample werd bedekt met zwart karton, met uitzondering van een lijn van 50×5 mm, op een zekere afstand van de meetzijde. Door deze opening werd het sample belicht met een blauwe of een groene LED. Deze LED's werden speciaal gekozen voor de experimenten met lumogen red, zij komen immers overeen met de golflengtes waar pieken in het absorptiespectrum terug te vinden zijn, en ze overlappen bovendien niet met het emissiespectrum, waardoor het LED-licht makkelijk van het luminescente licht te scheiden is.In figuur 1 vindt u een schematisch overzicht van de experimentele opstelling. De afstand tussen de belichte lijn, en de meetzijde werd gevarieerd, en voor elke afstand werd het luminescente spectrum opgemeten.

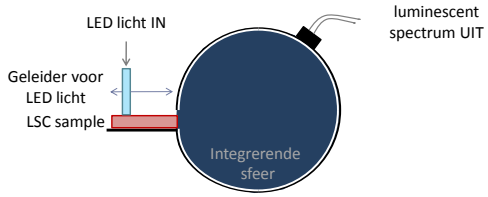

Fig. 1: Meetopstelling

B. Collectie-efficientie

De collectie-efficientie (η_{col}) is een getal dat alle verliezen uitdrukt, van het moment dat een foton voor het eerst geabsorbeerd wordt dooe een luminescente molecule tot het moment dat het licht uittreedt langs de meetzijde. Men bekomt de collectie-efficientie door de hoeveelheid licht die langs de meetzijde de LSC verlaat (aantal fotonen) te delen door de hoeveelhid licht geabsorbeerd door deluminescente materialen (aantal fotonen). De totale efficientie van het LSC systeem bekomt men door η_{col} tevermenigvuldigen met de absorptie efficientie (η_{abs}) en de externe efficientie van de fotovoltaïsche zonnecel (η_{PV}).

In figuur 2 ziet u de collectie-efficientie als functie van de afstand van de belichtingslijn tot de meetzijde. Deze is onafhankelijk van de golflengte van de lichtbron en neemt af met toenemende afstand tot de meetzijde. Deze afname wordt veroorzaakt

door de verliezen in de LSC.

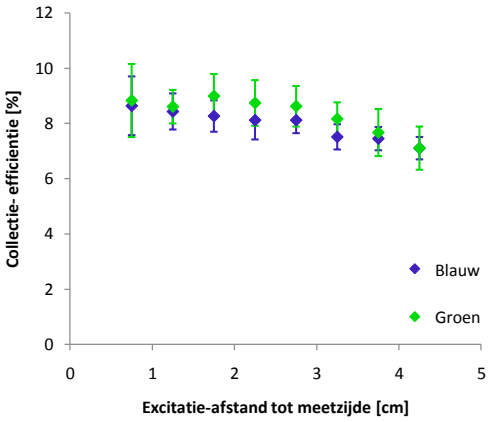

Fig. 2: collectie-efficientie als functie van de excitatie-afstand voor de blauwe en groene LED.

C. Reabsorptiewaarschijnlijkheid

De afname van de collectie-efficientie wordt veroorzaakt door allerlei soorten verliezen. De reabsorptiewaarschijnlijkheid (P_r) daarentegen is een specifieke maat voor reabsorptieverliezen. Ze is gerelateerd aan de overlevingswaarschijnlijkheid (P_0) als $P_0 = 1 - P_r$. De overlevingswaarschijnlijkheid is gedefinieerd als de kans dat een voor het eerst uitgezonden luminescent foton de meetzijde bereikt zonde op zijn weg gereabsorbeerd te worden.

De overlevingswaarschijnlijkheid is in figuur 3 uitgezet als functie van de excitatie-afstand.

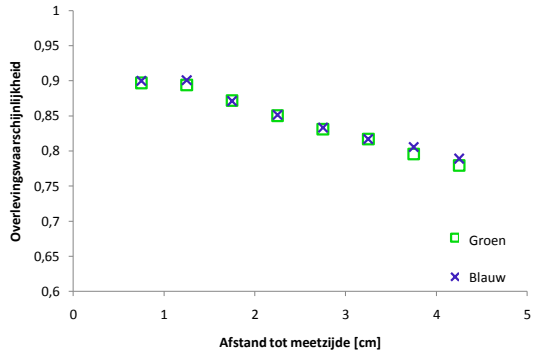

Fig. 3: Reabsorptiewaarschijnlijkheid als functie van excitatie-afstand voor blauw en groen LED licht.

III. Simulaties

A. LightTools, een simulatieprogramma gebaseerd op raytracing

Raytracing is een vaak gebruikte techniek voor simulatie van LSC's. In dit geval werd LightTools gebruikt als simulatieprogramma omdat het luminescente moleculen op een gedetailleerde manier kan integreren in de *raytracing* simulaties. Behalve de exacte eigenschappen van de zijkanten van het sample (speculair reflecterend, Lambertiaans scatterend, ...) waren alle parameters van de experimentele situatie gekend of konden ingeschat worden. De invloed van de eigenschappen van de zijwanden op de collectie-efficientie en de gemeten spectra werd vervolgens onderzocht.

B. Collectie-efficienties voor verschillende zijwanden

In figuur 4 ziet u de gesimuleerde collectie-efficienties voor verschillende eigenschappen van de zijwanden, samen met de experimentele waarden. De invloed van de zijwanden is, in het bijzonder voor de kleine sample-grootte die gebruikt werd, vrij groot. De simulatie genaamd complete scattering 3 ligt het dichtste bij de experimentele waarden. Voor deze simulatie werden de zijwanden zo gekozen dat ze 25% van het licht doorlaten, en 75% reflecteren. Zowel voor het doorgelaten als het gereflecteerde licht was de helft ervan Lambertiaans, en de andere helft quasi speculair (cos^5 distributie).

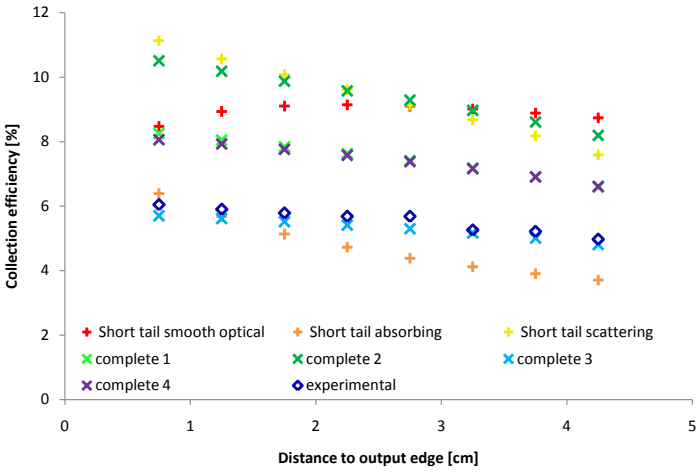

Fig. 4: Gesimuleerde en experimentele collectie-efficienties als functie van de excitatie-afstand voor blauw LED licht. (Voor deze figuur werd de energie van het licht (Watt) in plaats van het aantal fotonen gebruikt in teller en noemer van de collectie-efficientie)Simulated and experimental collection efficiencies as a function of excitation distance for the blue LED light.(In this case the energy of the light (Watt) is used in nominator and denominator instead of the amount of photons)

C. Spectra voor verschillende soorten zijwanden

De Gesimuleerde spectra waren in grote mate afhankelijk van de eigenschappen van de zijwanden. Het is door de verschillen in de output spectra dat ook de collectie-efficientie zo verschilt naargelang de zijwand. Het is inderdaad zo dat de eigenschappen van de zijwanden een onmiddellijkeinvloed hebben op de padlengte van het licht alvorens het de meetzijde berijkt. Langere padlengtes zorgen voor meer reabsorptie en hierdoor ook voor grotere reabsorptieverliezen.

Wij zijn in het bijzonder geïnteresseerd in de roodverschuiving van de spectra. Deze wordt veroorzaakt door reabsorptie van licht in de overlapregio aan de korte golflengtezijde van het emissiespectrum van het luminescent materiaal. Als deze roodverschuiving correct wordt gesimuleerd voor grote excitatie-afstanden, kunnen we aannemen dat de reabsorptie in de LSC correct gesimuleerd werd.

IV. Conclusies

De gebruikde experimentele opstelling kan verder ontwikkeld worden als een eenvoudig hulpmiddel om reabsorptieverliezen in LSC's te karakterizeren en te vergelijken. Er is nood aan de ontwikkeling van een extra opstelling om de eigenschappen van de zijwanden van de samples te bepalen. Als zo een opstelling gebouwd wordt kunnen de LightTools modellen vervolledigd worden, en kan het hierboven beschreven experiment gebruikt worden als een referentie voor de *raytracing* simulaties.

Referenties

[1] A. M. Hermann, *Luminescent solar concentrators, a review*, Solar Energy 29 (1982) 323-329.

[2] B. C. Rowan et al., *Advanced material concepts for luminescent solar concentrators*, IEEE journal of selected topics in quantum electronics 14 (2008) 1312-1322.

[3] M. G. Debye et al. , *Effect on the output of a luminescent solar concentrator on application of organic wavelength-selective mirrors*, Applied Optics 49 (2010) 745-751.

Contents

List of abbreviations and symbols

LED	Light emitting diode
LSC	Luminescent solar concentrator
PMMA	Poly(methyl methacrylate)
PV	Photovoltaic
QD	Quantumdot
QE	Quantum efficiency
QY	Quantum yield
RE	Rare earth
TIR	Total internal reflection
TU/e	Technical university of Eindhoven
UV	Ultraviolet

ΔE	Stokesshift. *eV.*
η	Efficiency.
η_{abs}	Absorption efficiency. *No units.*
$\eta_{coll,(p/E)}$	Collection efficiency, calculated based on photon or energy fluxes. *No units.*
$\eta_{opt,(p/E)}$	Optical efficiency, calculated based on photon or energy fluxes. *No units.*
θ_c	Critical angle. *Radians or degrees.*
σ	Standard deviation.
ω	Solid angle. *Sterradians.*
A	Area. m^2.
$Abs(\lambda)$	Absorption spectrum. Probability that light of a certain wavelength is absorbed. *No units.*
$c_{p/E}$	Effective concentration ratio. *No units.* expressed in terms of photon or energy fluxes.
$d\epsilon$	Element of étendue. *sterradians·*m^2.
$E_{0,(p/E)}$	Total amount of incident light. Incident spectrum integrated over all wavelengths. *W or photon flux.*
$E_{0,(p/E)}(\lambda)$	Incident spectrum. *W/nm or photon flux per nm.*
$E_0(\theta)$	Distribution of the incident light as a function of the angle of incidence θ.
$E_{abs,(p/E)}$	Absorbed light. *W or number of photons.*
$E_{dye,(p)}(\lambda)$	Luminescent spectrum emitted by the dye, without reabsorption.
$E_{edge,(p/E)}(\lambda)$	Luminescent spectrum measured at the measurement edge of the sample.
$E^{scaled}_{edge,(p)}(\lambda)$	Scaled edge spectrum.
$E_{LSC,(p/E)}$	Photon or energy flux incident on the luminescent solar concentrator. *Watt or number of photons.*
$E_{PV,(p/E)}$	Photon or energy flux incident on the photovoltaic cell. *Watt or number of photons.*
G_g	Geometrical gain. *No units.*
I	Current. *A.*
I_0	Incident Irradiance (flux/unit area). W/m^2.
$I_{LSC,(p/E)}$	Irradiance incident on the luminescent solar concentrator expressed in terms of photons or in terms of energy. W/m^2 *or number of photons per* m^2.
$I_{PV,(p/E)}$	Irradiance incident on the photovoltaic cell expressed in terms of photons or in terms of energy. W/m^2 *or number of photons per* m^2.
k	Boltzmann constant. $8.617343 \cdot 10^{-5} eV/K$.
L	Chance that light is lost through the loss conen. *No units.*
$MFP(\lambda)$	Mean free path for a certain wavelength. *mm*
n	Refractive index. *No units.*
P_0	Survival probability. $1 - P_r$.*No units.*
P_r	Reabsorption probability. *No units.*
$R_i, i = 1, 2, ...$	Generalized reflection coefficient at the i^{th} interface, for the specific incident distribution on that interface. *No units.*

R_p	Reflection coefficient for p-polarized light.*No units.*
R_s	Reflection coefficient for s-polarized light. *No units.*
SF	Scale function. *No units.*
t_{layer}	Thickness of the coated dye layer.*mm.*

Chapter 1

Introduction

It is expected that the energy demand will increase drastically in the 21st century. On the one hand the world population is steadily growing, on the other hand more and more people in developing countries are getting access to the welfare and technologies that were previously only available in the western world. In strong contrast with this increasing demand is the old-fashioned energy supply and distribution scheme that we are currently using. Being largely based on finite energy resources such as oil and gas, and posing problems concerning waste (e.g. CO_2, nuclear waste) and accessibility of remote areas, it is clear that this system as is will not be able to fulfill the growing needs of our population.

During the last few years, a lot of attention has been paid to renewable energy resources of all kinds. This goes from research efforts, over media attention to government regulations, policies and financial support and has resulted in a rapidly growing and very diverse renewable energy market, ranging from small to large scale and incorporating amongst others wind, biomass, geothermal, hydro-electricity and solar technologies.

Solar energy has the advantage of being a distributed technology. Unlike wind energy for example, which can only be applied on a large scale, solar energy installations can not only be found in huge solar farms, but also on individual peoples rooftops and even integrated in low-power consumer electronics. Installation of photovoltaic modules is considered to be the best way of bringing electricity to remote villages in developing countries. The largest drawback is the price, which is still too high to be competitive with other forms of energy without government incentives.

Projects have been set up (a.o. the FULLSPECTRUM project funded by the European commission [1]) that bundle research towards new solar technologies that use the solar spectrum in a more complete and efficient way. Luminescent solar concentrator (LSC) research also benefits from this driving force towards new and more efficient photovoltaic technologies.

The idea behind luminescent solar concentrators is to catch the light inside a transparent plate, by the use of luminescent materials. Those luminescent materials absorb the incident solar light and reemit it at a longer wavelength, after which it is guided towards the edges of the plate, where it is incident on small solar cells that are tailored to the wavelength range of the luminescent material. The light inside the plate is concentrated, so a much smaller area of photovoltaic cells is needed to obtain the same amount

of electricity. An additional advantage of luminescent concentrators compared to traditional concentrators is that they also capture diffuse light and don't have to use expensive tracking systems. [2]

Although in theory, high concentrations are possible [3], [4], they have until now not been reached in practice. Significant losses are caused by several mechanisms and their reduction is the most important focus of LSC research at this moment.

In this thesis work loss mechanisms in luminescent solar concentrators will be investigated in more detail. In particular, the reabsorption loss, which is caused by the overlap between the absorption and emission spectrum of the luminescent material is investigated booth through simulations and experiments.

In the next chapter the theory behind luminescent solar concentrators will be outlined. Attention will be paid to the working principle and the existing loss mechanisms, to the luminescent materials that can be used and to the photovoltaic cell which will be attached to the concentrator.

In chapter three all details about the experimental part of this work can be found. 50 x 50 x 5 mm poly (methyl methacrylate) (PMMA) plates with a red dye spincoated on top of it are studied both by measurements and simulations. The aim is to understand how reabsorption affects the emission at one side of the sample as a function of the excitation distance to that side. Both the setup and the results are described in detail.

The entire fourth chapter is devoted to simulations. In this chapter an outline of the different simulation possibilities for luminescent solar concentrators can be found, as well as more details about the method and software used for this work and the obtained results.

The last chapter contains the conclusion of this thesis work as well as some recommendations for future research.

Chapter 2

Luminescent solar concentrators

Already in 1973 a first solar collector system based on a solution of laser dye between two glass plates was constructed by Lerner, however his ideas were rejected by the National Science Foundation [5], and it was only three years later in 1976 that the first paper on the topic was published by Weber and Lambe [6]. Subsequently the subject gained popularity very quickly with several groups all over the world doing research on luminescent concentrators for solar applications.

Despite the fact that the theory was very promising and a lot of progress was made in the first years, the poor performance of the luminescent materials at that time hindered further advances. It would take almost 20 years before researchers regained interest in the subject thanks to new developments in materials such as quantum dots, new theoretical insights and a strong drive to make solar energy cheaper by using the solar spectrum more efficiently.

In this chapter the operation principle of LSCs is described in detail. The first section will be devoted to the concentrating system itself, its general working principle and the materials it consists of. A short discussion of photovoltaic cells, the way they work and how they can be adapted to use with luminescent concentrators is the subject of the second section.

2.1 Principle of operation

2.1.1 General

A luminescent concentrator basically consists of a transparent plate which either contains luminophores (fluorophores or phosphors) or is coated with a layer containing them in a stronger concentration. The transparent plate is usually a glass or PMMA plate. The sunlight incident on the plate is partly absorbed by the luminophores and subsequently reemitted at a longer wavelength. Most of this luminescent light is kept inside the glass plate by total internal reflection. At one or more edges of the concentrator small photovoltaic cells are attached that absorb the luminescent light when it arrives at that edge and convert it into electricity.

Other components can be added to improve the efficiency of the system. Anti reflection coatings, both on the photovoltaic cell and on top of the concentrator plate, mirrors or lambertian reflectors at the edges that are not used by solar cells and at the bottom,

ultraviolet (UV) filters if the dye is known to degrade under UV-light, and wavelength selective filters to keep also the luminescent light that is not totally internally reflected inside the concentrator are some examples of such components.

To characterize the performance of luminescent solar concentrators the effective concentration ratio is defined as the irradiance (photon- or energy flux per unit area) incident on the solar cell divided by the irradiance on the LSC. This concentration ratio can also be rewritten as a product of the optical efficiency, which is the ratio of the output and the input fluxes and can also be expressed in terms of photons or energy, and the so called geometrical gain, defined as the ratio of the LSC top area and the area of the attached photovoltaic cell.

$$\begin{aligned} c_{(p/E)} &= \frac{I_{PV,(p/E)}}{I_{LSC,(p/E)}} \\ &= \frac{E_{PV,(p/E)} A_{LSC}}{E_{LSC,(p/E)} A_{PV}} \\ &= \eta_{opt,(p/E)} G_g \end{aligned} \tag{2.1}$$

In this equation p and/or E between parentheses in the subscript denotes the usage of photon- and/or energy fluxes respectively, a convention that will be used further throughout this work.

Luminescent solar concentrators are not only used in photovoltaic systems, they also find applications in daylighting systems. LSC stacks with different color dyes are employed to guide sunlight inside buildings. In this application color perception of the outcoming light is the more important characteristic, rather than the amount of energy that can be transmitted to the edge. [7],[8].

2.1.2 Loss mechanisms

Not all the incident light reaches the solar cell; there are several other things that can happen. This subsection will try to give a complete description of the possibilities. Two schematic representations can be found in figures 2.1 and 2.2.

First of all the incident light is not entirely absorbed by the luminescent material. A portion of it is reflected at the interface between the air and the concentrator(figure 2.1.a), and even the light that enters is not necessarily absorbed. The sunlight has a very broad spectrum, while most luminophores only absorb light in a much smaller wavelength range. By comparing the absorption spectrum of the luminophore with the incident spectrum, you get an idea about the amount of light that can be absorbed and in which wavelength range. This amount is quantified in what is called the absorption efficiency:

$$\eta_{abs} = \frac{\int E_{0,(p/E)}(\lambda) Abs(\lambda) d\lambda}{\int E_{0,(p/E)}(\lambda) d\lambda} \tag{2.2}$$

with $E_0(\lambda)$ the incident spectrum(in Watt or number of photons per nm) and $Abs(\lambda)$ the absorption spectrum of the dye (figure 2.1.b).

The absorption of light by a molecule brings the latter in an excited state. It can subsequently return to the groundstate either via radiative (send out a photon) or non-radiative transfer(figure 2.1.d). The chance that the molecule returns to its ground state

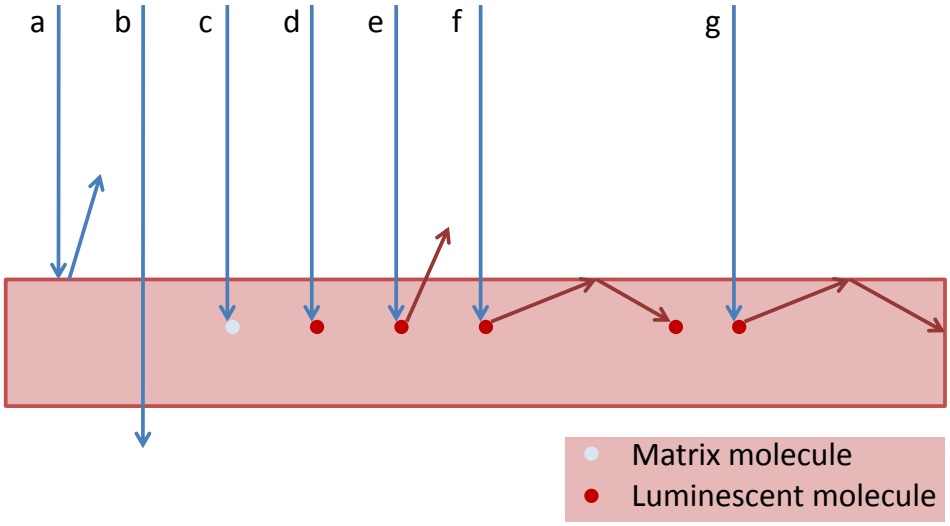

Figure 2.1: Schematic representation of the processes that can happen to light incident on an LSC. a: Reflection at the air-LSC interface; b: Light that is not absorbed; c: Light that is absorbed by a matrix molecule; d: Light that is absorbed by a luminescent molecule but not reemitted; e: Light that is emitted in the loss cone of the concentrator; f: Light that is totally internally reflected and reabsorbed by another luminescent molecule; g: luminescent light that reaches the edge of the concentrator.

through sending out a luminescent photon is called the luminescent quantum yield(QY) or quantum efficiency(QE). Luminophores often have preferred emission directions, but because of their random orientation in the concentrator the total emission of luminescent photons is more or less uniform in all directions. Every luminescent photon always has an energy equal to or lower than the initially absorbed photon. The emission spectrum will therefore be red shifted compared to the absorption spectrum. This shift is often called the Stokes shift.

The light is kept inside the concentrator via total internal reflection (TIR) (figure 2.1.f/g). At the interface from an optically more dense to an optically less dense medium light which is incident on an angle larger than a certain critical angle θ_c is completely reflected. The critical angle can be calculated according to Snell's law:

$$\sin(\theta_c) = \frac{1}{n} \tag{2.3}$$

Where air is taken as the optical least dense medium and n is the refractive index of the optically more dense medium, this is typically around 1.5 for glass and PMMA. the cone defined by this critical angle is called the loss cone(figure 2.1.e). The chance that the light that has been emitted by the luminophores is lost through the loss cones (both at the top

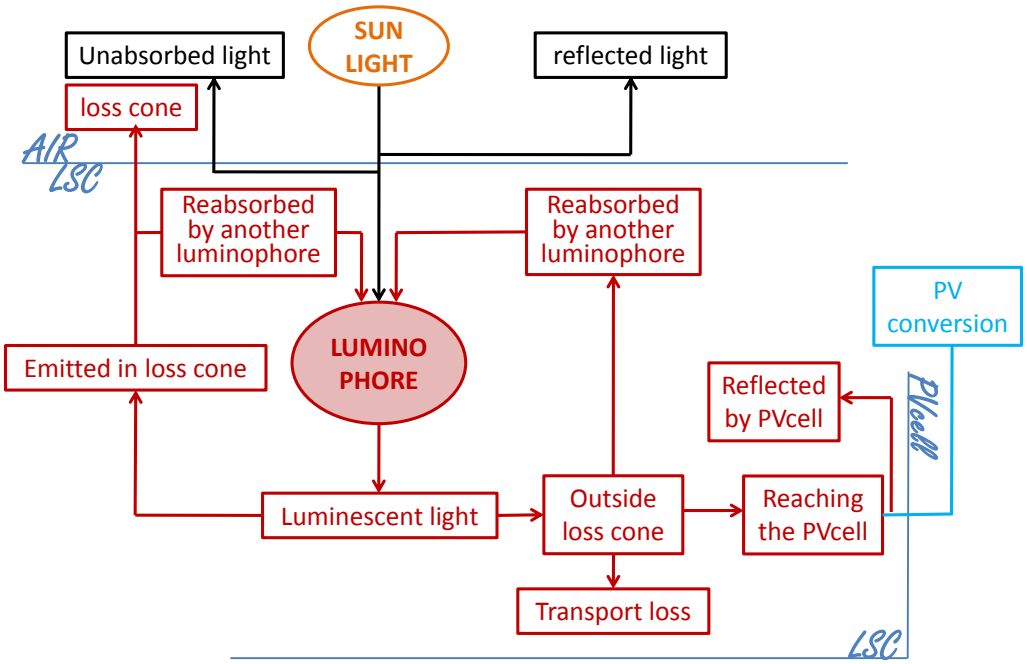

Figure 2.2: Diagram representing the important processes taking place in an LSC.

and at the bottom) is calculated below.

$$\begin{aligned} L &= \frac{lost\ solid\ angle}{total\ solid\ angle} \\ &= \frac{2\int_0^{2\pi}\int_0^{\theta_c}\sin(\theta)d\phi d\theta}{4\pi} \\ &= 1-\cos(\theta_c) \\ &= 1-\frac{\sqrt{n^2-1}}{n} \end{aligned} \tag{2.4}$$

For $n = 1.5$, $L = 0.2546$. If the plate is not completely flat this loss can be even larger.

Light that is not lost through the loss cone can reach the output edge and be absorbed by the photovoltaic cell(figure 2.1.g), reach another edge and be lost, or if there is a mirror at that edge, be reflected back into the concentrator according to the properties of the mirror, depending on the quality of the matrix material (usually glass or PMMA) it can also be absorbed by the matrix and be lost, and last but not least, it can encounter another luminophore and be reabsorbed. For this to happen the wavelength of the light needs to be in the overlap region between the absorption and emission spectrum. The light that is reabsorbed will again encounter the quantum efficiency of the dye, a Stokes shift, and can again be lost through the loss cone. It can be expected that reabsorption will play an important role in the total loss of the system.

Figure 2.2 gives a more abstract representation of the processes taking place in the LSC. By giving every arrow in this diagram a certain probability, the overall efficiency and the importance of the different loss mechanisms can be calculated. However this wil

get complicated very soon because of the feedback loops and the wavelength dependence of the probabilities. For this reason simulation programs are of great importance in the study of luminescent solar concentrators.

2.1.3 Theoretical limits

Besides the loss mechanisms described above it is of course not possible to concentrate light endlessly. This subsection describes the theoretical limits of solar concentrators.

Normal concentrating systems are limited by the law of conservation of optical étendue which is valid in all lossless optical systems. An element of étendue is defined as [9]:

$$d\varepsilon = n^2 \cos\theta d\omega dA \tag{2.5}$$

With n the refractive index of the medium the beam is passing through, θ the angle between the propagation direction of the beam and the normal, $d\omega$ the divergence of the beam and dA its surface. The maximum concentration of the number of photons in such a system equals thus:

$$c_{(p)}^{max} = \frac{A_1}{A_2} = \frac{\Delta\omega_2}{\Delta\omega_1} n_2^2 \tag{2.6}$$

where $\theta_1 = \theta_2$ and $n_1 = 1$ is supposed. In the case of diffuse incoming light (large $\Delta\omega_1$), the maximal concentration factor of normal solar concentrators is on the order of n_2^2, which is particularly low. On the other hand, concentration can be high if the incident light has small divergence. This is why normal geometrical concentrators work with tracking systems in order to receive light directly from the sun, rather than diffuse light.

The strength of luminescent concentrators lies in the fact that they are not lossless and thus don't have to obey the above law of conservation of étendue. However they still obey the laws of thermodynamics, according to which the maximal concentration is enhanced by a factor $Fe^{\Delta E/kT}$, with ΔE the Stokes shift and F a factor taking into account the internal processes. A precise derivation can be found in [10]. Even Stokes shifts on the order of 0.2 eV give concentration factors of almost 3000 at room temperature. [4], [11]

The main idea of LSCs is thus the ability to concentrate even diffuse light on the sacrifice of an energy loss in the Stokes shift. In the work of Zastrow [12], a simplified model is used to make this idea more understandable (see figure 2.3). The model consists of a box containing fluorescent molecules that absorb blue light and emit red light. Blue light enters the box through a blue filter at the left, while red light can leave the box through a red filter at the right. If the input and output ports have the same size, no concentration takes place; however, if the output port is made smaller while the size of the input port is conserved, light will be concentrated, as the same amount of red photons is now leaving through a smaller port. This concentration is limited, because at a certain moment the larger amount of red light inside the box will saturate the population of the exited state of the luminescent molecules, and they will no longer emit red light. Also, the concentration cannot take place without the presence of the Stokes shift.

Huge concentrations are possible if all losses described in the previous subsection can be overcome, and ongoing research is all about overcoming as much losses as possible.Therefore, a lot of attention is paid to the production of luminescent materials that can be used for this purpose.

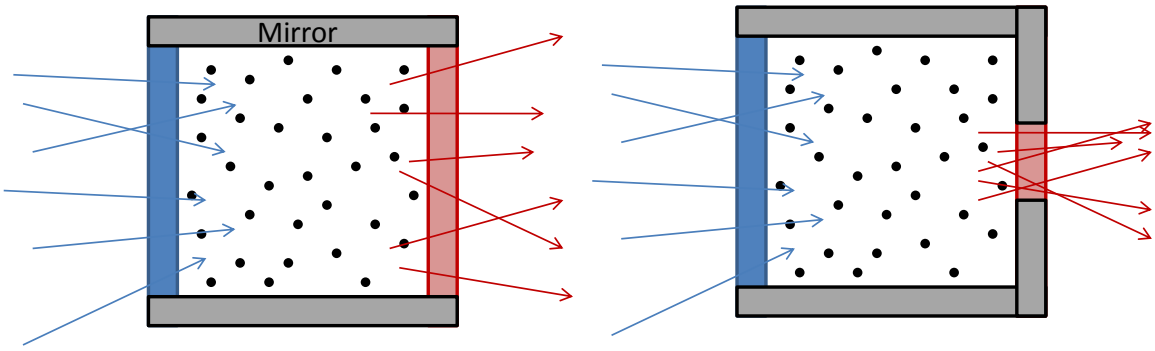

Figure 2.3: Simplified model to explain the concentration of light by a luminescent solar concentrator. From [12].

2.1.4 Luminescent materials

Luminescent materials for LSCs should have certain properties in order to lead to an efficient concentrating system. These properties include a broad absorption range, with high absorption efficiency, a near unity luminescent quantum yield, an emission spectrum tailored to the bandgap of the used photovoltaic cell, no or small overlap between absorption and emission spectrum to prevent reabsorption, and long-term stability under outside weather circumstances.

In order to fulfill those requirements different material classes have been explored:

Organic materials

Organic dyes where the first luminescent materials used in LSCs, they generally have high quantum yields and are relatively inexpensive compared to inorganic fluorescent dyes. Some of them are also found to be quite stable if protected from additives and/or UV-light. However, they have a large overlap between absorption and emission spectra, causing large losses due to reabsorption.[13]

Semiconducting polymers are originally developed for the light-emitting diode industry. They often have very high quantum yields and also their lifetimes can be long. When polymers are excited, they undergo a change in structural conformation, which has a positive effect on the Stokes shifts and may thus reduce reabsorption losses. Moreover, the width of their absorption and emission bands can be tuned by controlling the chain lengths. [14]

Inorganic materials

Rare earth materials and quantum dots are recently explored for use in LSCs, they are both promissing materials for several reasons.

Rare Earth(RE) materials have the advantage of reduced reabsorption because they either emit to energy levels above the ground state or upon excitation, decay radiationless to a level that cannot be excited directly. However they have low absorption

coefficients, which means that large amounts are needed. They can also be combined with well absorbing (organic) materials that can transfer their energy to the RE materials in order to be viable LSC candidates [15].

Quantum dots on the other hand could be advantageous because of their tunability. They can be synthesized in different sizes to obtain desirable absorption and emission spectra. Also the width of the absorption and emission bands is related to the size distribution, so overlap can be avoided by producing quantum dots which have a small size distribution. QDs may present high quantum yields and long lifetime, although quantum dots combining the desired properties for LSCs are not yet commercially available. [14]

None of the materials that are currently available exhibit all the desired characteristics. Combinations of different existing materials and the search for new materials could lead to a breakthrough at this point. The results of LSC material research will be determinative for the future of luminescent concentrators.

2.1.5 Advanced configurations

Stacked configurations

If one wants to cover the complete solar spectrum with the absorption of the LSC it is very likely that more than one dye will be needed. The dyes can be combined in one plate, but this has the disadvantage that dyes with a lower quantum efficiency (for example: a dye in the near infrared with a high QY has not yet been found) will introduce a lot of extra losses. Concentrator stacks have been proposed as a good way to create broad absorbing LSCs [16], [17], [18], [19]. Either the longest or the shortest wavelength dye is put on top; if absorption regions of dyes overlap, the dye with the highest luminescent quantum yield is put above the one with the lower QY. A mirror or diffuse reflector is often placed under the stack to give the light that has not been absorbed a second chance. An extra feature is that different solar cells with band gaps adjusted to the emission bands of the specific dyes can be placed at the edges.

Photonic bandgap filters

Photonic bandgap filters are used to minimize the escape cone losses inherent to LSCs. Ideally they have a reflection coefficient that is one for the luminescent wavelengths and zero for all other wavelengths (especially the wavelengths in the absorption band of the used luminophores). However, because the reflection coefficient will always be angular dependent, also part of the incoming light which could otherwise be absorbed by the dye will be reflected by such a structure. Moreover, the optimal position of the reflection band is not always clear, since often a trade-off has to be made between reflecting as much of the luminescent light as possible, and not blocking too much of the useful incoming light. Until now, mirrors have been produced that existed either of a 1D multilayer photonic structure, of 3D photonic structures such as opals [20], or of cholesteric nematic liquid crystals [21]. Optimizations of the different structures is still needed to obtain near 100% reflection in a band with a sharp cutoff. If the costs can be kept low, a stacked LSC with photonic bandgapfilters applied is the most probable candidate for commercialization. An example of such a combined stack is given in figure 2.4.

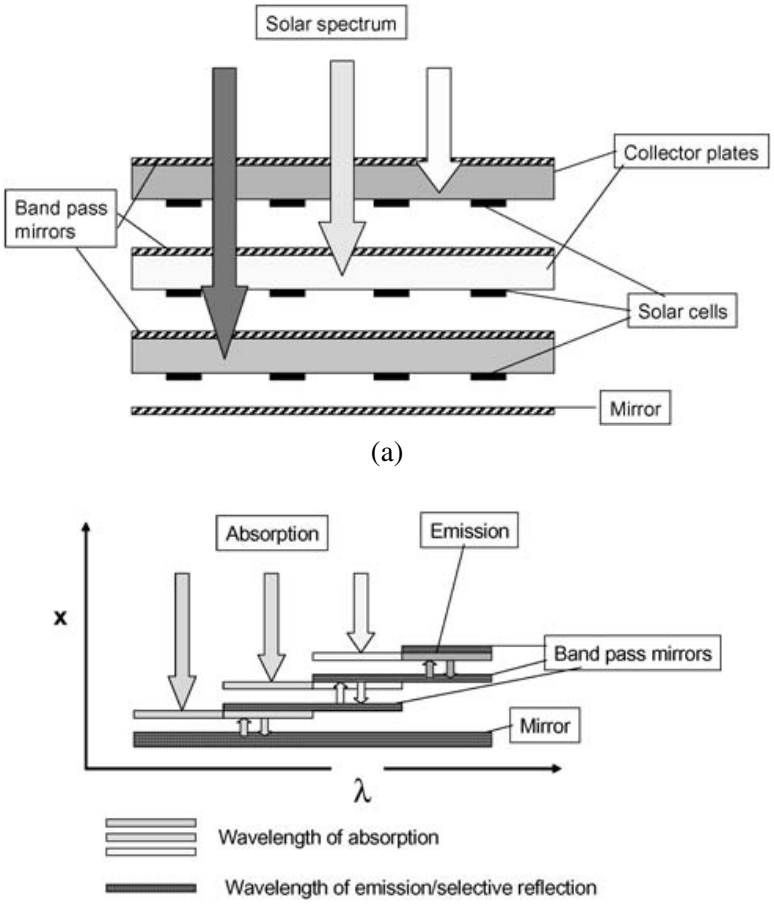

Figure 2.4: Luminescent solar concentrator stack with bandgap filters. Geometrical representation (a) and wavelength representation (b). [16]

Upconverters and downconverters

Upconverters are compounds that combine several lower energy photons to a higher energy photon. When an upconverter is placed under an LSC, on top of a mirror, it can improve the efficiency by upconverting low energy light that is not absorbed to higher energy photons that are sent back into the concentrator and can be absorbed by the luminophores.

Downconverters split high energy photons in two lower energy photons. Similar to upconverters, they can be used to downconvert high energy photons that pass through the concentrator without being absorbed to lower energy photons that can be absorbed by the luminescent material.

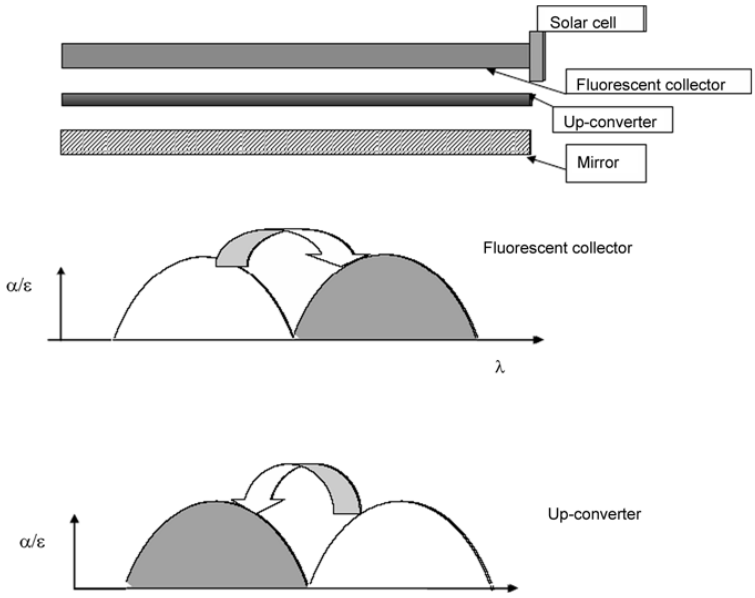

Figure 2.5: Combination of an LSC and an up-converter.[16]

Dye alignment

The absorption and emission of many dyes is related to there structure. They often have preferred directions for absorption and/or emission, a phenomenon that can be used to improve the output of luminescent solar concentrators if the molecules can be aligned macroscopically. This can often easily be done using liquid crystals as a host material. Aligned dyes have been shown to improve the trapping efficiency by sending less light into the loss cone [22]. They can also be used to improve the irradiance from certain edges, making it possible to have highly efficient concentrators with photovoltaic cells only at those edges that are favored by the aligned dye (figure 2.6). [23]

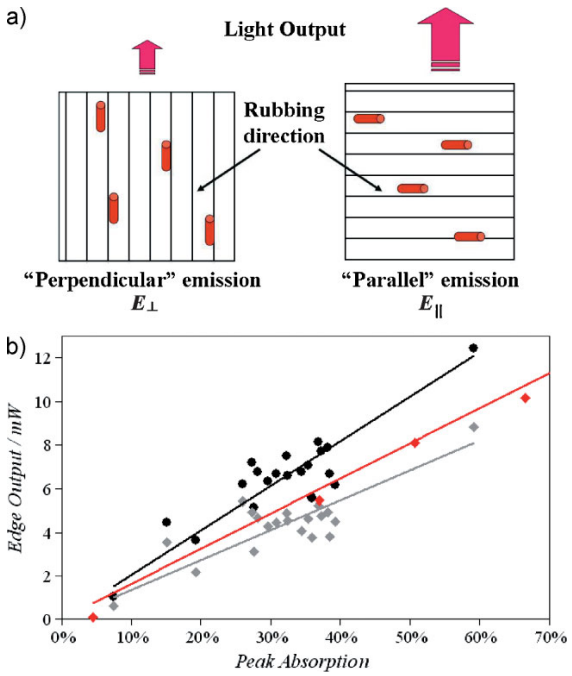

Figure 2.6: a) Representation of 2 samples with aligned dye molecules. The red cylinders represent the dye molecules. b) Integrated edge emission as a function of the absorption for isotropic layers (red), parallel alligned layers(black) and perpedicularly alligned layers (gray). [23]

2.2 Photovoltaic cell

Luminescent solar concentrators are used together with solar cells. It is the combination of the concentrator and the photovoltaic cell that will determine the overall efficiency and cost. For this reason, an introduction to photovoltaic cells is also part of this introductory chapter about LSC systems. This section is however limited to the basics and will not talk about the new developments in photovoltaics such as thin film and dye sensitized solar cells.

Photovoltaic cells consist mainly of a semiconductor material in which a p-n junction is introduced. At both sides of the junction metal ohmic contacts are attached. This is schematically shown in figure 2.7.

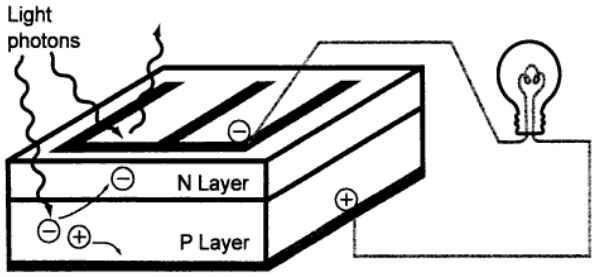

Figure 2.7: Schematical representation of a photovoltaic cell.[2]

When photons with an energy larger than the bandgap of the semiconductor are absorbed by the solar cell, electron hole pairs are formed. Thanks to the electric field introduced by the p-n junction, holes will be accelerated towards one electrode, and electrons towards the other (figure 2.8). In this way a current is generated.

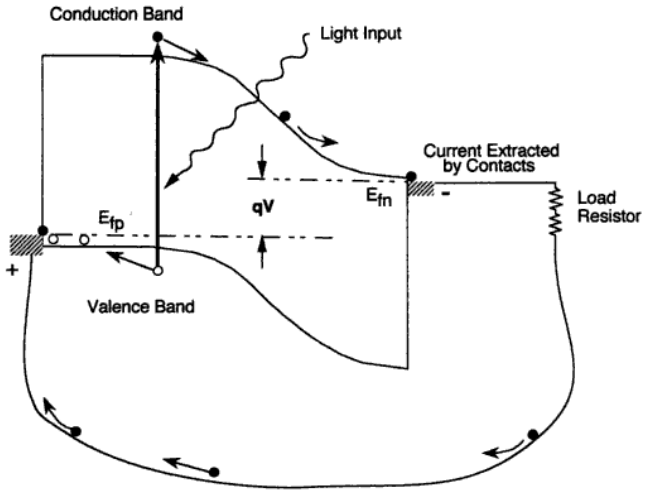

Figure 2.8: Energy band structure with the generation of electron hole pairs in a photovoltaic cell. [2]

In electrical engineering equivalent electrical circuits are often used. The circuit used to represent the physical processes inside a photovoltaic cell is given in figure 2.9 The current voltage characteristic associated with this circuit is can be writen as:

$$I = I_0 \left[exp\left(\frac{qV}{nkT}\right) - 1 \right] - I_L \tag{2.7}$$

and is drawn in the graph in figure 2.9. It is nothing more than a diode characteristic that is shifted downwards with an amount I_L. This is understandable because the solar cell can be seen as a large area diode with an extra current generated by the incoming photons. It must be noted that this is a representation of an ideal situation and that some effects such as the extra losses at the edges and due to non ideal contacts are not taken

into account. These losses can be represented by an extra series and shunt resistance in the equivalent circuit. [24]

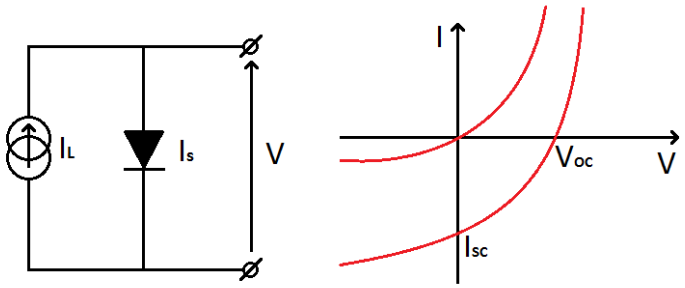

Figure 2.9: Current-voltage characteristic of an ideal photovoltaic cell. I_L is called the light current, I_S the current through the diode, V_OC is the open circuit voltage and I_SC the short circuit current.Taken from [24].

Simple solar cells cannot use the entire solar spectrum efficiently. Photons with energies lower than the bandgap of the semiconductor are not absorbed, and of photons with an energy larger than the bandgap, only the bandgap energy is converted to electricity and the remainder is converted to heat. In luminescent solar concentrators the spectrum incident on the solar cell will be determined by the dye used. The attached solar cell can than be chosen to have a bandgap appropriate for use with that particular dye. A number of semiconductors with their bandgap energies are depicted in figure 2.10. Although only a small photovoltaic cell area is needed for LSCs, it is good to keep in mind that some semiconductor materials are quite expensive.

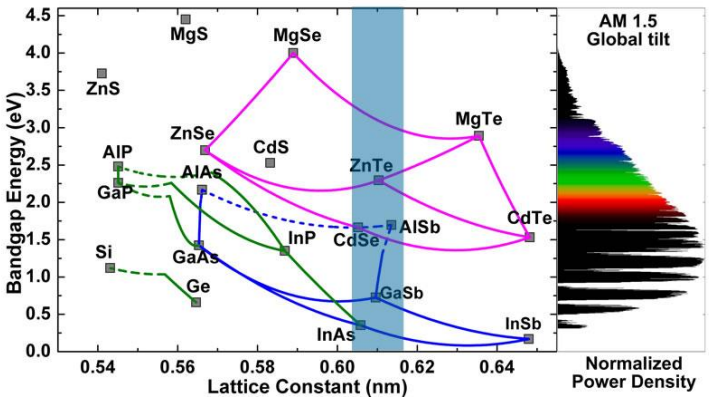

Figure 2.10: Band gap energies of different semiconductors. [25]

Another advantage of concentrating the light before it is incident on a solar cell is that the efficiency (together with the open circuit voltage) of photovoltaic cells initially increases logaritmically with the incident flux. At even higher fluxes, internal loss mechanisms and higher solar cell temperatures lower the efficiency again.[26], [27] The result is the peaked curve that can be seen in figure 2.11.

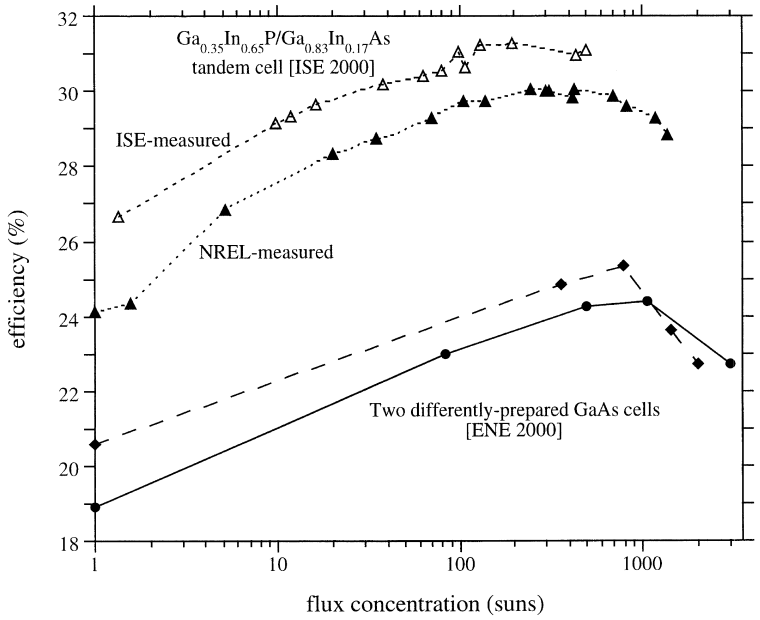

Figure 2.11: Efficiency as a function of irradiance (in number of suns: one sun corresponds to the standard illumination at AM1.5 or 1 kW per square meter) for different photovoltaic cells. [27]

Chapter 3

Measurements

3.1 Sample preparation

We choose to study Lumogen F Rot 305 (figure 3.1), an organic dye manufactured by BASF, because it is often used in luminescent solar concentrator prototypes and demonstrators. Although the dye has a large photoluminescent quantum yield, is quite stable and has a relatively broad absorption band; it is certainly not perfect. The main drawback for use in large scale solar luminescent concentrators is its large overlap between the absorption and emission spectrum. Light that is emitted at a wavelength in this overlap region risks to be reabsorbed by another dye molecule. With each absorption there is a chance that the photon is lost either through the loss cone or because of the non-unity quantum yield.

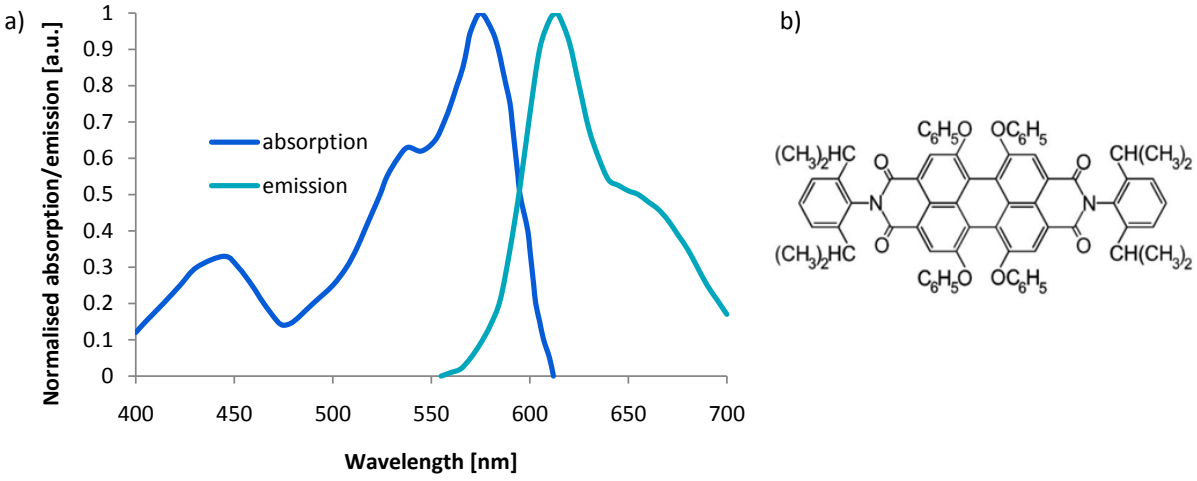

Figure 3.1: a) Normalized absorption and emission spectrum of the lumogen red dye [28]. b) Chemical structure of the lumogen red dye [29].

Samples are prepared by spincoating the dye on top of blank PMMA plates. In theory, for samples that are large enough, it is expected that the results with spincoated samples are similar to those of samples which have the dye dispersed in the PMMA plate itself if a

correction factor for the difference in thickness between the plate and the coating is taken into account for the concentration. However there are a few reasons why there could be differences in practice.

First of all concentration quenching occurs at higher concentrations of the dye. This issue should be taken care of because a lower quantum efficiency caused by quenching will make the reabsorption losses worse. [30]

The spincoated layer will also not be perfectly smooth, which will have an influence on the total internal reflection and the loss cone related to the top surface.

Also the behavior of light emitted close to the edges is different. Two typical examples of such edge effects are illustrated in figure 3.2. In the left two pictures, a particular ray is drawn, which is reabsorbed in the case of a filled sample and reaches the output edge in the case of a coated sample. Once reflected at the bottom of the waveguide, the ray in the coated sample never gets the chance to be reabsorbed again because it will not reach the dye layer, while in the filled waveguide the dye is all over (but in a smaller concentration) and the ray does get the chance to be reabsorbed after reflection at the bottom of the sample. The illustrations at the right of figure 3.2 show a ray that is lost through the bottom of the filled sample, but reaches the output edge in the case of the coated sample. This only makes a difference if this ray is also able to get out, for example because the edges are lambertian scatterers instead of perfectly smooth surfaces.

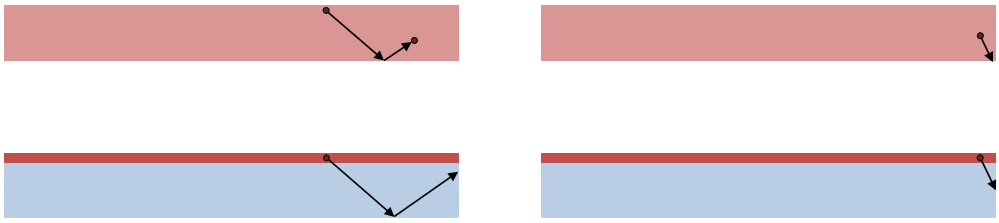

Figure 3.2: Illustration of the differences near the edges between filled and coated samples.

Finally, due to its structure (large, flat), the dye molecule may have a preferred direction when coated in such a thin layer. Where in bulk, the emission and absorption of this dye are assumed to be independent of the angle of incidence or emission because of the random orientation, if coated, there might be preferred directions for absorption and/or emission.

Although the above mentioned differences are often at the disadvantage of the coated samples, we choose to use those because of the ease with which coated samples can be produced at the TU/e lab facilities.

The PMMA plates are 5 mm thick and are cut manually in pieces of 5 cm by 5 cm. The cut edges are not polished and are thus not 100% smooth. Examination of the sample edges by eye learns that they are not very scattering as well. We assume that the samples are mostly specular reflective, with some scattering.

Samples were painted black at one edge and measurements were done at the opposite edge unless indicated otherwise. By doing this, light rays that would otherwise be reflected at the back edge and reach the front edge after having traveled a much longer pathlength are eliminated and a better correlation between the excitation distance and the actual pathlength traveled by the light before reaching the edge is created.

We choose not to paint the side edges because this would make the fraction of the solid angle of the emission of a dye molecule that can reach the output edge dependent on the distance of this excited molecule to that edge.

3.2 Measurement set-up

3.2.1 General

The measurement set-up (depicted in figure 3.3) uses an integrating sphere with a sample holder and a spectrometer. The sample lies on the sample holder which is a 50×50 mm table facing a 5×49 mm hole in the sphere. It is illuminated by an LED source consisting of a number of LEDs coupling their light in a PMMA waveguide, which can be put on top of the sample.

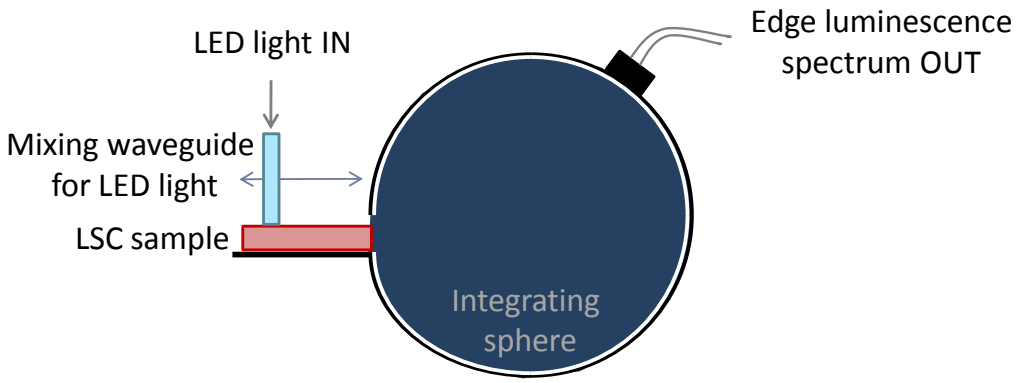

Figure 3.3: Representation of the experimental set-up.

Two sources were made based on the same principle but with different LEDs (figure 3.4). The first source uses 5 blue Rebel high power LEDs from Philips Lumileds (peak wavelength at 447 nm). The second source uses 2x7 side emitting low power multicolor LEDs from Nichia (peak wavelengths at 625 nm 524 nm and 456 nm for red, green and blue respectively). The angular dependence of both LED types is approximately lambertian. The LEDs are attached to 1 edge of a $50 \times 50 \times 5$ mm PMMA plate of the same type as was used to prepare the samples. The opposite edge is placed on the sample to perform the measurement. The red from the multicolor LED is not used, the spectra from the other LED sources are shown in figure 3.5.

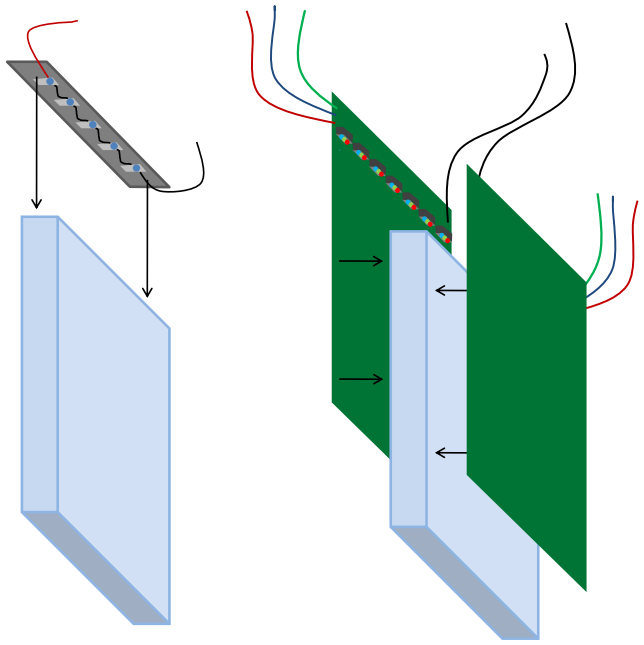

Figure 3.4: LED source consisting of 5 Rebel high power LEDs (left) and LED source consisting of 2x7 side emitting LEDs (right).

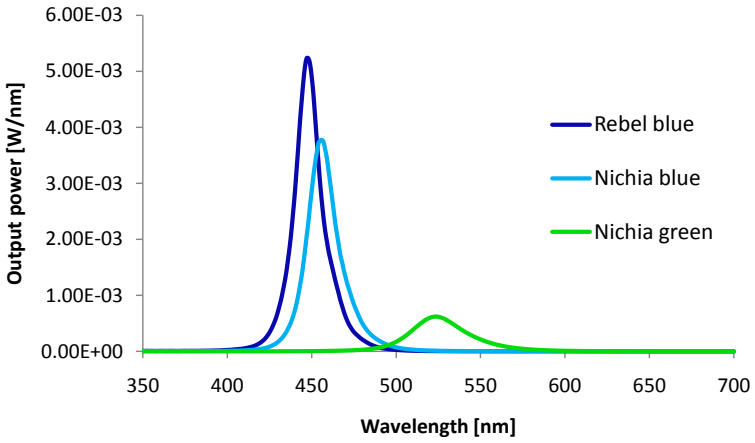

Figure 3.5: Measured spectra of the LED sources.

To prevent stray light from the source to reach the sample a black piece of cardboard with a 50×5 mm hole for the LED sources in it are placed on top of the sample.

3.2.2 From theory to practice: some important considerations

The measurement setup which is described in the above section was realized at Philips Research using the available equipment. In October 2010 a first setup was build, incorporating an Ocean Optics spectrometer, an integrating sphere, a custom made sample holder and a first blue LED source with Rebel high power LEDs from Philips Lumileds. The calibration of the spectrometer was done using another setup with integrating sphere

and calibrated Labsphere detector. Later it was decided to excite the dye also using the absorption peak in the green, so a second LED source was added. Because this source used three color side emitting LED arrays, another blue light source had also become available by this.

However, measurements done with the first setup seemed inconsistent. After controlling every step in the experiment and the calculations it was concluded that the linearity between different exposure times of the spectrometer was insufficient for our measurements. We decided to use the Labsphere setup which was already calibrated (the same we had used to calibrate the first setup).

At this stage the first blue source (the one with the rebels) broke down (one connection and one LED were broken). Because of the availability of blue LEDs on the other source as well, it was decided not to repair the first source, but to continue the measurements with the other one.

By the time the final good measurements were done in January, we had gained a lot of knowledge about building this kind of setup and about the components we had worked with. This knowledge has no influence on the final results but may be useful for other people planning to set up similar experiments. This section is dedicated to this information and may thus be skipped by readers who are merely interested in the obtained results.

The source

In this subsection both the current/voltage source and the LED sources will be discussed. The choices of these two devices are not independent of each other. When using a high power LED which is fed by 100 mA for example, a resolution and accuracy of 1 mA for the current supply may be good enough, but when working with low power LEDs it is better to choose a more accurate supply. In our experiments, finally a Keithley 2420 3A Sourcemeter was used. This was certainly sufficient for the used LEDs.

In the beginning the LED source was turned off after every measurement to prevent it from heating up. Later I learned that it is better to turn the LEDs on some time before the measurement to let the heating stabilize and to leave it on during the whole experiment.

The graph in figure 3.6 and table 3.1 illustrate that the LEDs are more stable when they are not turned off and on every time. The results were obtained by a series of 16 measurements with 1 minute between each measurement. Table 3.1 also shows the importance of LED stability by comparing the LED fluctuations to the mean edge luminescence output of a sample that is illuminated by this LED at 2.5 mm from the output edge.

The detector

Calibration

The USB2000+VIS/NIR is a miniature fiber optic spectrometer from Ocean Optics. It consists of a grating which projects different wavelengths of the incoming light onto different pixels of a CCD array (figure 3.7). The spectrometer comes with a software package

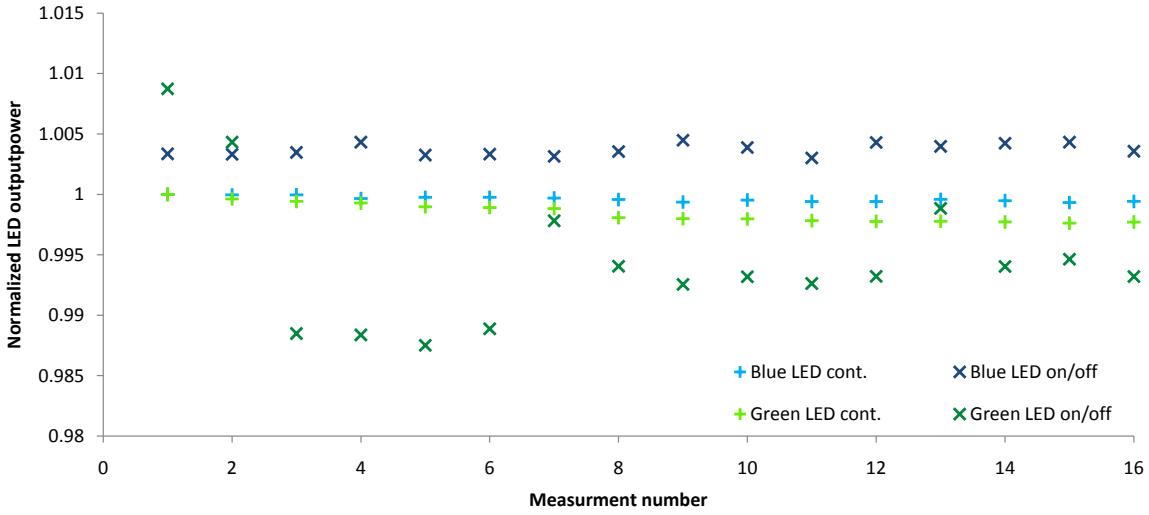

Figure 3.6: Source stability measurement for the blue and green LED sources.

Table 3.1: Stability of the LED sources.

	average output power [W]	2σ	2σ relative to average output power [%]	2σ relative to average luminescent power [%]
Blue LED cont.	9,70E-02	4,28E-05	0,04	3,26
Blue LED on/off	9,74E-02	9,52E-05	0,10	7,23
Green LED cont.	2,88E-02	4,65E-05	0,16	6,43
Green LED on/off	2,87E-02	3,32E-04	1,16	45,88

which allows amongst others to select the exposure time and the number of spectra averaged, to subtract a dark spectrum and to view the spectra on a graph with the wavelength on the horizontal and the number of counts at the corresponding pixel on the vertical axis.

The horizontal axis is expected to be already calibrated. This is checked by measuring the peaks of a TL-lamp both in a calibrated set-up and with the uncalibrated detector. The agreement is quite good, as can be seen in figure 3.8.

The vertical axis is not calibrated. The number of counts of the pixel belonging to that particular wavelength is returned by the software and this number of counts is wavelength dependent. The sensitivity of silicon detectors is not at all constant in the wavelength range of the spectrometer (350 nm-1000 nm). The typical response curve of this silicon detector is depicted in figure 3.9

This axis can be calibrated towards a number of photons or towards optical power, but both can be easily converted into each other. In this case the spectrometer was calibrated towards power, because the reference spectrometer that we will use for the calibration returns power spectra. Calibration is done by measuring a 10W halogen lamp driven by a fixed voltage and current, both in the calibrated set-up and in the uncalibrated one.

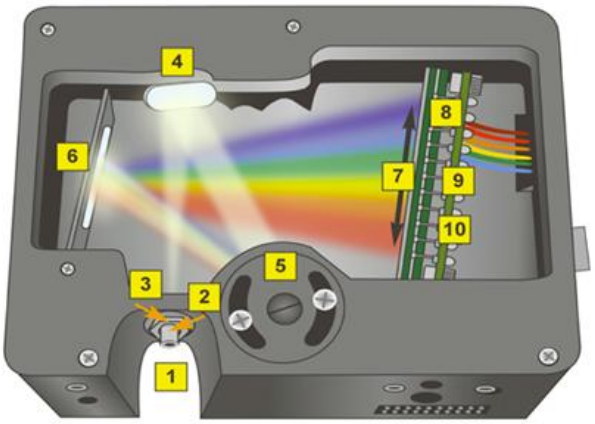

Figure 3.7: Working mechanism of ocean optics USB 2000+ spectrometer. 1) SMA 905 connector, 2) fixed entrance slit, 3) Longpass absorbing filter (optional), 4) collimating mirror, 5) grating, 6) focussing mirror, 7) detector collection lenses (optional), 8) Detector, 9) OFLV variable longpass order sorting filter (optional), 10) UV detector upgrade (optional). [31]

A calibration function can be defined which, upon multiplication with an uncalibrated spectrum has the calibrated spectrum as a solution. The halogen lamp spectra measured in both set-ups as well as the calculated calibration function are shown in figure 3.10. From those graphs it can be understood that this calibration procedure will add a lot of noise at short and at long wavelengths.

This simple multiplication with the calibration function suffices if the same exposure time is used all the time. In our case however, both the light source and the luminescence at the edge of a sample caused by exciting it with the same light source will have to be measured. Therefore the use of different exposure times will certainly be needed. Another factor will have to be multiplied with the obtained spectrum to take this into account. For example if the exposure time is doubled, the detector will make twice as much counts and thus the spectrum with the longer exposure time will have to be divided by two to become comparable to the other one.

Linearity

Different things can be meant when speaking about linearity. First of all one can mean the linearity between different measurements using the same exposure time but measuring different signals of which one covers less of the total possible power before saturation of the detector than the other one. If this linearity is low, measurements always have to be done at such exposure times that the detector is used at the same portion of its saturation.

On the other hand the linearity between different exposure times is also not always perfect. This can be caused by transient phenomena on short time scales for electronic shutters or due to the final time needed to open and close the shutter which is not correctly taken into account. Other causes may also be possible. In this case it is not possible to

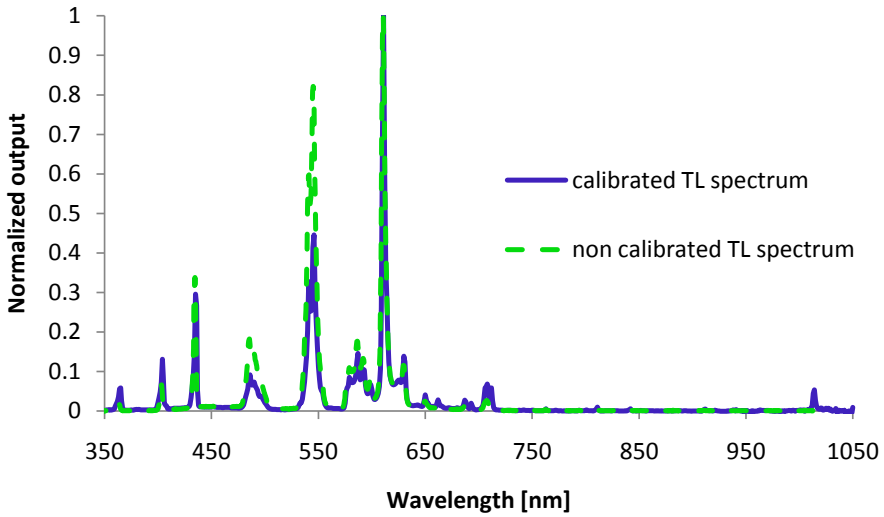

Figure 3.8: Spectrum of a TL-lamp measured with a calibrated and uncalibrated detector to check wavelength calibration of the latter.

compare signals measured at different exposure times.

In both cases the non-linearity can be corrected for if its shape is known. In order to measure this, a known light source and a set of known attenuators can be used. If the correction has to be done over a large dynamic range, this requires a lot of time and effort.

In our measurements we measured the different LED sources and the luminescence they caused when exciting a LSC sample at different distances from the output edge. We multiplied the spectra of the sources with the absorption spectrum of the dye to obtain the amount of light that was absorbed by the sample. Later we divided the total amount of luminescent light by the total amount of absorbed light to obtain a quantity called the collection efficiency (more detailed information about the collection efficiency can be found in section 3.3.1). This collection efficiency was measured and calculated for the different sources (the blue high power source and the green and the blue low power side emitter source). Against our expectations different efficiencies were obtained for the different sources; even for the two blue sources the results were significantly different from each other (figure 3.11).

To check the linearity the same signal was measured at different exposure times. It turned out that even with the small differences in exposure times that we could measure with one source and without saturating the detector the relationship was not linear. We presumed that the deviations could be even larger when the factor between the exposure times for the compared measurements exceeds one hundred as was the case in the calculations of the collection efficiency. Indeed the different sources have different intensities (figure 3.5) and had thus been measured at different exposure times (and so was the luminescence they caused). Especially the difference between the blue high power LED source and the blue and green from the low power side emitting source is large. The blue

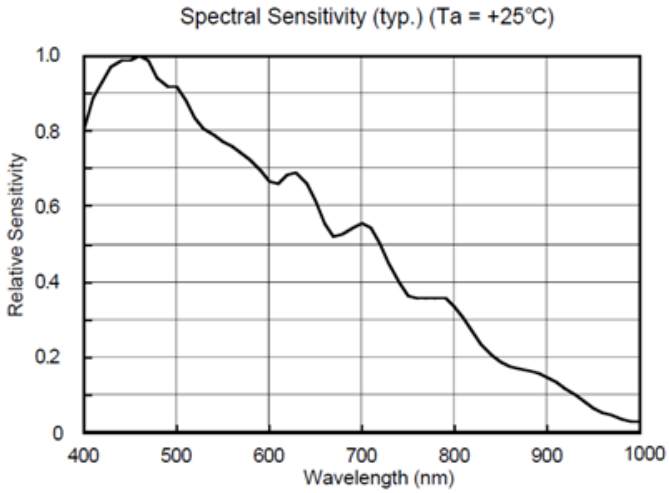

Figure 3.9: Sensitivity of the Sony ILX 511 2048 pixel CCD linear detector used in the Ocean Optics USB 2000+ spectrometer. [32]

and green from the low power source had intensities that could be measured at the same exposure time although the green source will in that case cover a smaller portion of the saturation of the detector. By repeating the measurements of one particular measurement point again, while taking care of using the same exposure times for the blue and the green source the assumption that the non-linearity between the different exposure times was the cause of the inconsistency between the measurements was confirmed.

At this point we decided to redo the experiments with the setup we had until now only used to calibrate the Ocean Optics spectrometer. This set-up was known to be calibrated and linear up to 5% (value from the Labsphere detector manual).

3.3 Results

3.3.1 Fluorescence collection efficiency and optical efficiency

Definition and calculation

In literature ([12], [15], [16], [33]), the optical efficiency is defined as the amount of luminescent light coming out of the used edges of an LSC divided by the amount of light incident on the plate. The amount of light can be expressed as a number of photons per time unit, or as an energy flux in Watt. Depending on which quantity is used we talk about photon to photon or Watt to Watt optical efficiency.

Because the spectrum of the LED source is not at all comparable with the solar spectrum it is in the case of our experiments better to use an efficiency which only incorporates what happens from the moment that the light is absorbed by the dye for the first time. We call this efficiency the collection efficiency. It is defined as the amount of light emitted

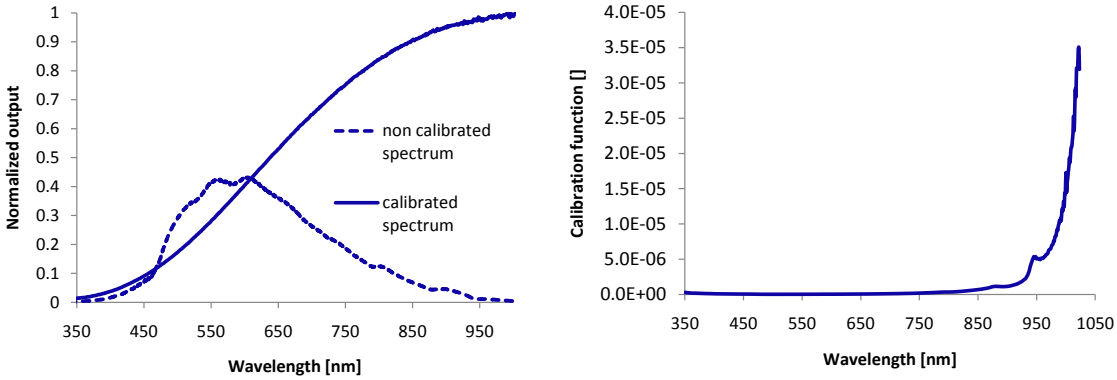

Figure 3.10: Spectra of a halogen lamp taken with a calibrated and the uncalibrated spectrometer (left) and the calibration function calculated from these spectra (right).

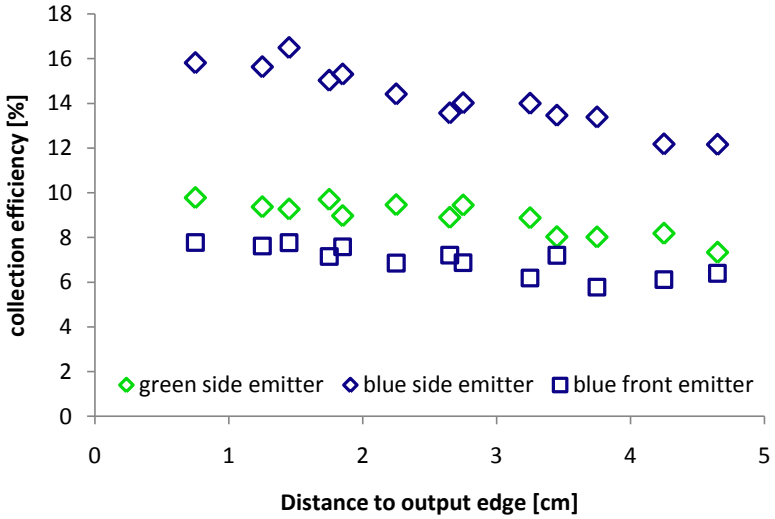

Figure 3.11: Graph representing the unexpected results of the measurements of the collection efficiency.

at one edge, the measurement edge, divided by the amount of light absorbed by the dye. If now this collection efficiency is expressed in terms of photons the excitation spectrum should not have an influence on the obtained result.

The absorption of the dye coating is measured with a Perkin Elmer Lambda 950 UV/VIS spectrometer. The intensity and spectrum of the LED sources is measured using the integrating sphere set-up (figure 3.3). With those spectra (figure 3.12) and assuming that the source is a lambertian emitter, the amount of LED light absorbed by the dye layer can be calculated.

A schematic representation of the situation is given in figure 3.13. The first order approximation in the generalized reflection coefficients of the amount of absorbed light can be written as:

$$E_{abs} = \eta_{abs}(1 - R_1 + R_2 - R_2\eta_{abs})E_0 \tag{3.1}$$

In this equation, E_{abs} denotes the total amount of absorbed light, E_0 the total amount of

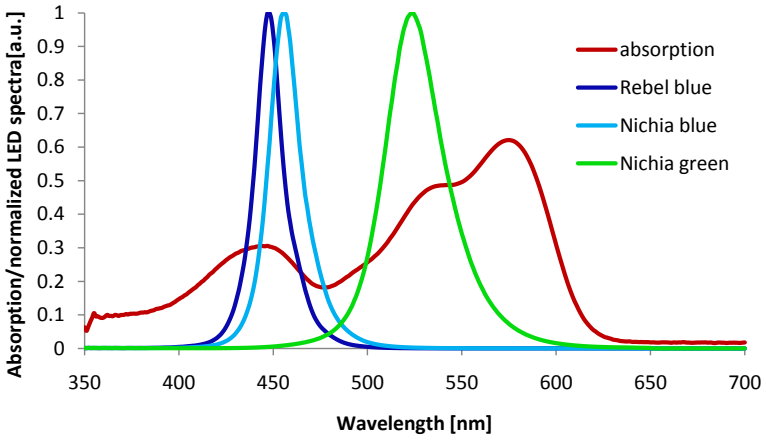

Figure 3.12: Absorption of the dye layer and normalized LED spectra on one graph. (Only the Nichia blue and green LEDs were used for final measurments)

incident light and η_{abs} the absorption efficiency for that particular incident spectrum and absorbing dye. This absorption probability can be calculated as followed:

$$\eta_{abs} = \frac{\int E_0(\lambda) Abs(\lambda) d\lambda}{\int E_0(\lambda) d\lambda} \tag{3.2}$$

The generalized reflection coefficients R_1 and R_2 take into account the Fresnel reflection for the specific angular profile that is incident on that particular interface. They can be calculated from the Fresnel equations.

$$R_s = \left[\frac{n_1 \cos\theta_i - n_2 \sqrt{1 - \left(\frac{n_1}{n_2} \sin\theta_i\right)^2}}{n_1 \cos\theta_i + n_2 \sqrt{1 - \left(\frac{n_1}{n_2} \sin\theta_i\right)^2}} \right]^2 \tag{3.3}$$

$$R_p = \left[\frac{n_1 \sqrt{1 - \left(\frac{n_1}{n_2} \sin\theta_i\right)^2} - n_2 \cos\theta_i}{n_1 \sqrt{1 - \left(\frac{n_1}{n_2} \sin\theta_i\right)^2} + n_2 \cos\theta_i} \right]^2 \tag{3.4}$$

For unpolarised light following the average coefficient applies:

$$R = \frac{R_s + R_p}{2} \tag{3.5}$$

The graph in figure 3.14 applies those equations on a lambertian profile incident on an air/PMMA interface($n_1 = 1$, $n_2 = 1.5$). The Fresnel reflection coefficient as well as the angular distribution of the reflected and transmitted light are displayed.

The graph in figure 3.15 does the same for the PMMA/air interface at the bottom of the plate. The normalized profile of the transmitted light through the air/PMMA interface from the previous calculation is used as input.

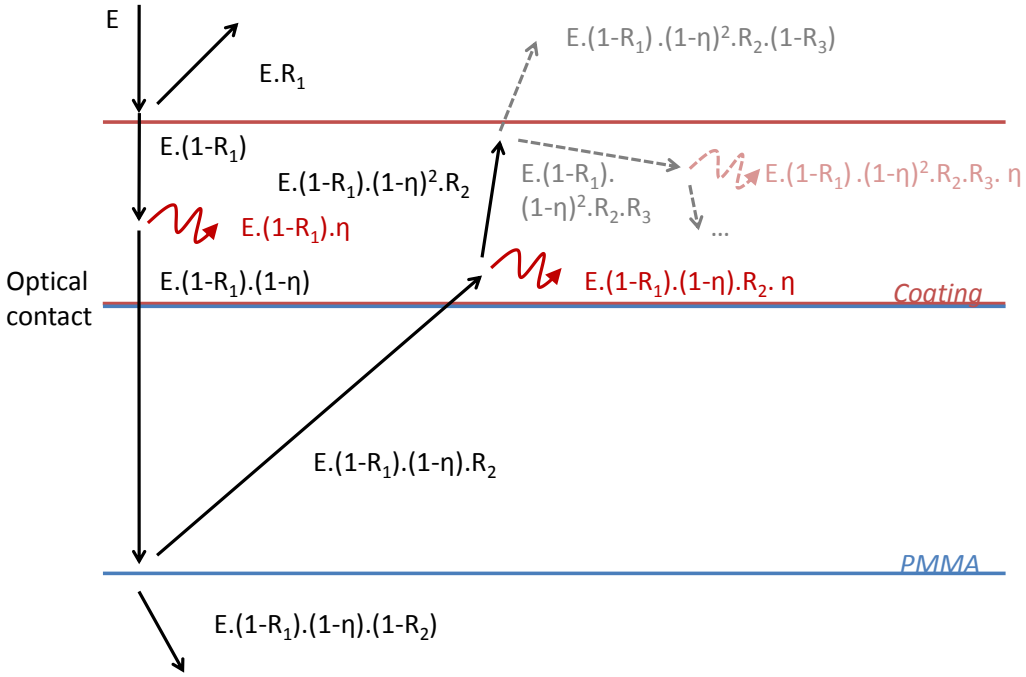

Figure 3.13: Schematical representation of the multiple reflections of the incoming LED light before it gets absorbed. In the calculations terms that are quadratic or higher order in a generalized reflection coefficient are omitted.

By integration of the reflected light over all angles and normalizing the result the two generalized reflection coefficients can be calculated:

$$R_1 = \frac{\int E_0(\theta) R(\theta) d\theta}{\int E_0(\theta) d\theta} = 0.068 \tag{3.6}$$

$$R_2 = \frac{\int E'(\theta) R'(\theta) d\theta}{\int E'(\theta) d\theta} = 0.061 \tag{3.7}$$

The collection efficiency can finally be calculated as follows:

$$\eta_{coll} = \frac{E_{edge,(p/E)}}{E_0 \eta_{abs} \left(1 - R_1 + R_2 - R_2 \eta_{abs}\right)} \tag{3.8}$$

And the relation between the optical efficiency and the collection efficiency is given by

$$\eta_{opt} = \frac{E_{abs}}{E_0} \eta_{coll} = \eta_{abs} \left(1 - R_1 + R_2 - R_2 \eta_{abs}\right) \eta_{coll} \tag{3.9}$$

Result

The spectra resulting from the illumination of a completely coated sample with the blue and green LED source at 8 measurement points at distances from 0.75 cm to 4.25 cm away from the measurement edge are given in figure 3.16. The absorption efficiencies can be calculated by using equation 3.2 and the spectra from figure 3.12.

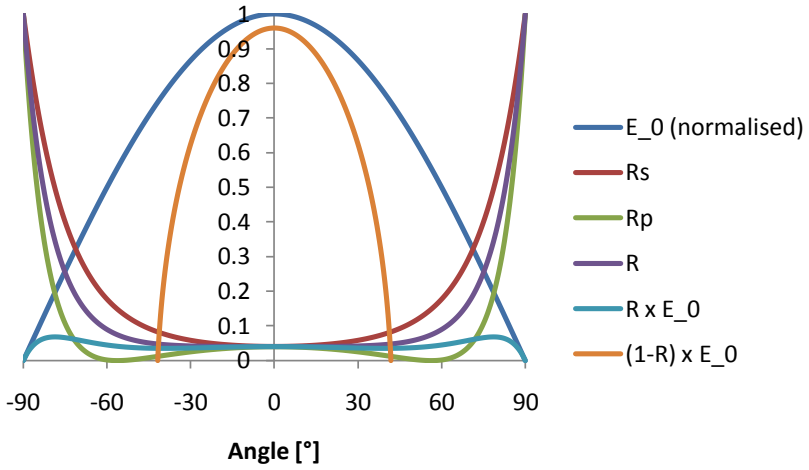

Figure 3.14: Fresnel reflection and transmission of Lambertian profile for an air-PMMA transition.

Integrating the incident and luminescent spectra and using equation 3.9 delivers the collection efficiency for every measurement point. They are depicted in figure 3.17. As expected the collection efficiency is lower for measurement points that are further away from the output edge. This is because the light has more chance to be reabsorbed several times before leaving the concentrator via the measurement edge when the excitation is further away from it. The typical redshift of the luminescent spectra when the distance to the measurement edge increases, illustrated in figure 3.18 by the evolution of the peak wavelength of the measured spectra as a function of this distance, confirms this.

We must admit that the peak wavelength is not the optimal, most objective way of measuring the red shift and thus the reabsorption. The change of this peak wavelength is indeed dependent on the form of the luminescence spectrum even if the absorption spectrum is the same. A better way to characterize reabsorption is by defining a reabsorption probability, which is done in the following subsection.

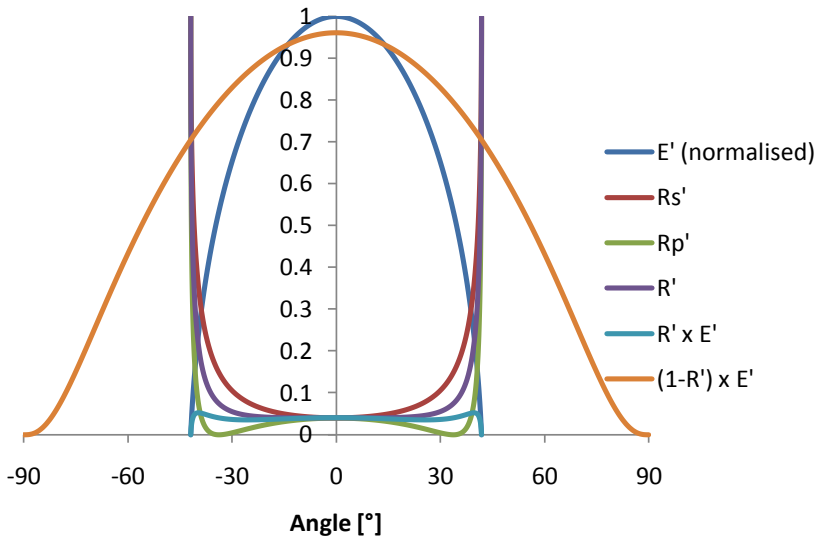

Figure 3.15: Fresnel reflection and transmission of the transmitted profile from figure 3.14 for an PMMA-air transition.

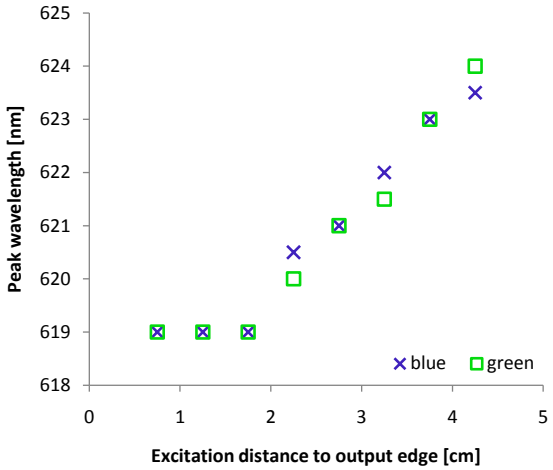

Figure 3.18: Peak wavelengths of the luminescent spectra as a function of the excitation distance both for excitation with blue and green light.

3.3.2 Reabsorption probability

Definition and calculation

The estimation of the reabsorption probability is based on the measurement of the edge spectra and a so called first time emission spectrum. This first time emission spectrum can be obtained from a sample with a very small concentration of luminescent dye, from a sample where the area that is covered by luminescent material is small, or both smaller dye concentration and coverage area.In this case we measured a sample with a 5×5 mm area of the same thickness and concentration of the dye on top of it in transmission.

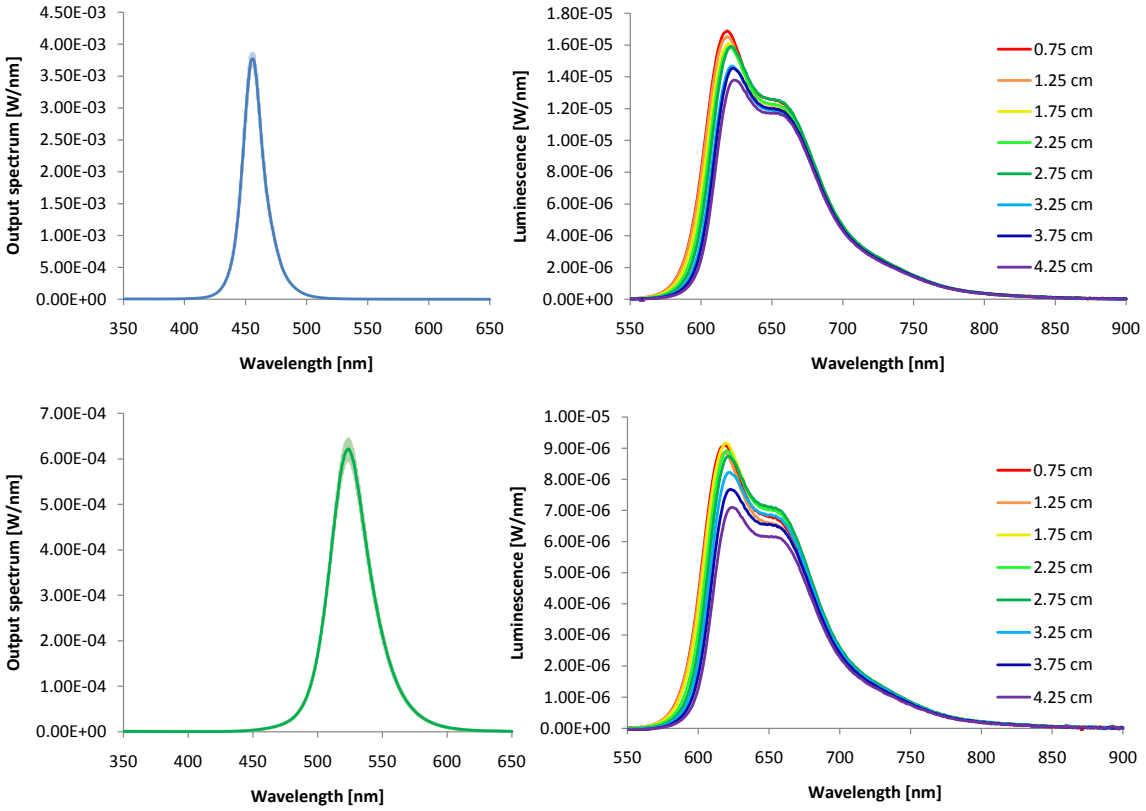

Figure 3.16: Blue/green LED spectrum(upper/lower left), the light blue/green background represents a 2σ error estimate on 10 measurements, and luminescence spectra as function of excitation distance(upper/lower right).

Additionally all side edges were painted black to prevent reabsorption after reflection at those edges. The same source is used for excitation, the luminescent power measured will be very weak, so the spectrum will be more noisy.

First, the survival probability P_0 is defined as the chance that a luminescent photon that was generated by excitation with the source (first time emission) will reach the detector without suffering reabsorption. The reabsorption probability $P_r = 1 - P_0$ is than the probability that a first time emission luminescent photon is reabsorbed on it s way to the output.

To obtain P_0 and thus also P_r we start from the fact that the long wavelength tale of the emission spectrum is free from reabsorption because at these wavelengths there is no overlap with the absorption spectrum anymore. We then scale the edge emission spectrum, such that its long wavelength tale coincides with the long wavelength tail of the first time emission spectrum. Rather than doing this scaling by eye, we make use of a scale function. This function is obtained by dividing the edge emission spectrum by the first time emission spectrum.

$$SF = \frac{E_{edge,(p)}(\lambda)}{E_{dye,(p)}(\lambda)} \tag{3.10}$$

With $E_{edge,(p)}(\lambda)$ the edge emission spectrum and $E_{dye,(p)}(\lambda)$ the first time emission spec-

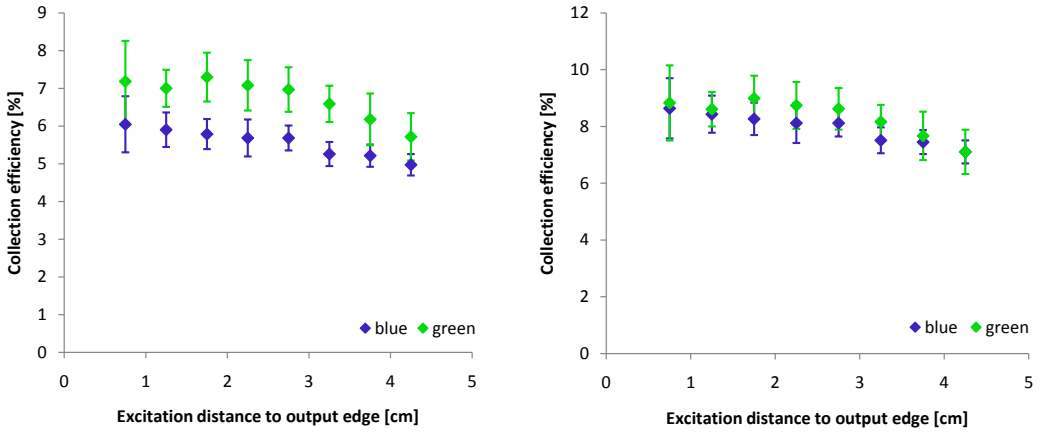

Figure 3.17: Watt to Watt (left) and photon to photon collection efficiencies as a function of excitation distance both for excitation with blue and green light, with 2σ error estimates.

trum of the dye. The scale function will become flat from the point where there is no reabsorption anymore. The ordinate of this flat line can be used as a scale factor by which E_{edge} has to be divided. The different spectra are depicted in figure 3.19. The horizontal line to the scale function was fitted for λ from 700 nm to 750 nm. The fact that the scale function is not flat anymore above 750 is probably due to the high noise of the original first time emission spectrum and the division of 2 low numbers, with a relatively high error to obtain the scale function.

Now P_0 can be calculated as the ratio of the area under the scaled edge emission spectrum and the area under the first time emission spectrum. [29], [34]

$$P_0 = \frac{\int E^{scaled}_{edge,(p)}(\lambda)d\lambda}{\int E_{dye,(p)}(\lambda)d\lambda} \tag{3.11}$$

Note that in this section we are always talking about photon spectra and not about energy spectra.

Result

We use the same edge emission spectra as we have used for calculating the collection efficiency. The resulting survival probability as a function of the excitation distance to the output edge is given in figure 3.20

The uncertainty on the survival probabilities plotted in 3.20 is expected to be relatively large for two reasons. The method for measuring the first time emission spectrum is not optimal, which leads to a noisy signal with already a large uncertainty. On top of that, the method of calculating the scale function leads to the division of 2 small numbers at the tail of the spectra. Due to this, the scale function can only be used between 700 and 750 nm, to obtain the scale factor. The use of this rather small wavelength interval can again introduce errors. A good estimate of the error is however difficult to make, and therefore, no error bars are depicted in figure **??**.

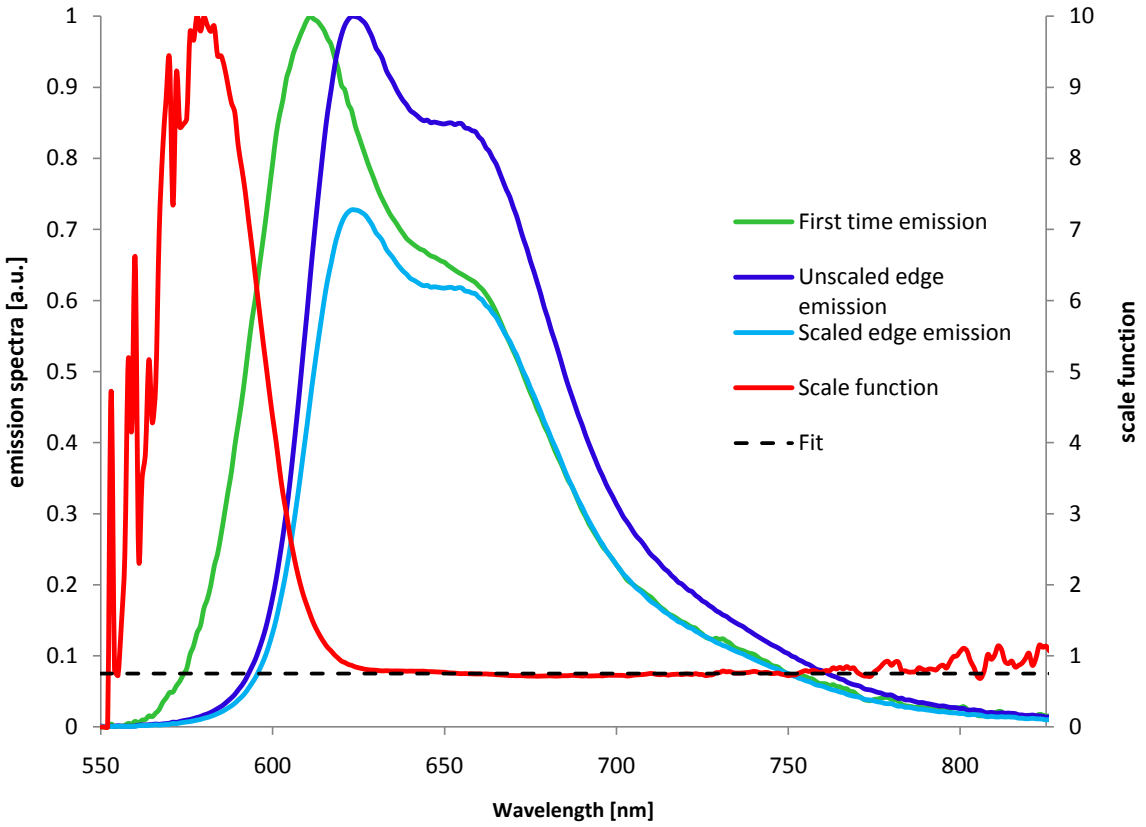

Figure 3.19: Graphical representation of the scaling procedure. The normalised edge emission spectrum(dark blue) is clearly red shifted compared to the first time emission spectrum(green). The scale function (red) is then succesfully used to obtain the scaled edge emission spectrum(light blue).

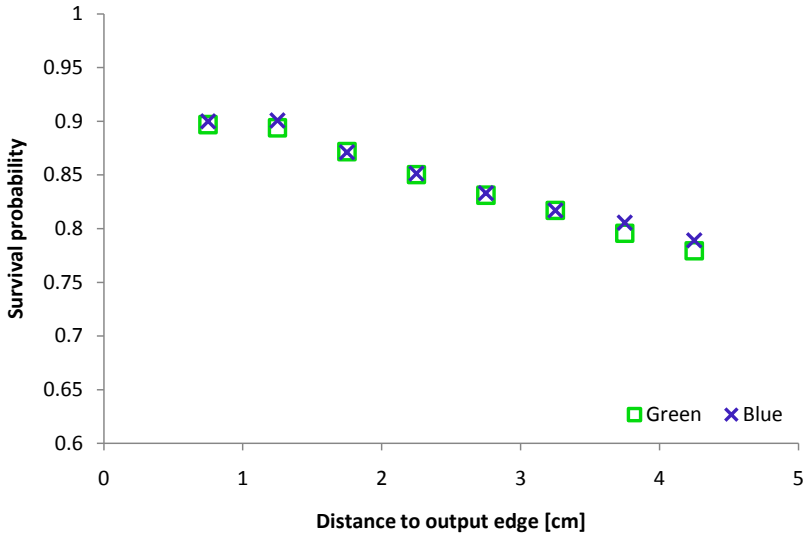

Figure 3.20: Survival probability as a function of excitation distance to output edge for excitation with blue and green LED.

Chapter 4

Simulations

Computer modeling has become a very important tool in optimization of the design parameters of LSCs. Therefore it is important to have models that incorporate all the processes in a correct and precise way. In this chapter the computer simulations of the experimental measurements from the previous chapter will be described. The first two sections introduce the different possibilities for simulating LSCs and also some details about the ray-tracing tool we are using. The third section describes the simulations results.

4.1 Different approaches

There are two approaches to LSC modeling: thermodynamic modeling and ray-tracing. Recently also a hybrid method that combines the possibilities of thermodynamic modeling and ray-tracing has been reported [35].

In thermodynamic modeling the radiative energy transfer between different points of a mesh is calculated. Detailed balance arguments relate the absorbed light to the spontaneous emission.Although this method relies on more simplifying assumptions than ray-tracing methods, this way of simulating allows to evaluate simple rectangular LSCs under direct sunlight in a relatively quick way. [35], [36]

Ray-tracing on the other hand is more flexible, it can model various geometries both under direct and diffuse illuminating conditions. It is a statistic model in which rays are used to represent light of a certain wavelength and with a certain direction. At each point where there are different possibilities, the fate of the ray is determined by means of random numbers. To be able to determine what could realistically happen to a ray the program needs a lot of input parameters such as the absorption and emission spectra of the dye and its quantum yield, but also the spectrum and angular distribution of the light source, the reflectivity of the edges etc. The statistical nature of this kind of simulations also means that lots of rays needs to be traced in order to obtain an output with low noise, which makes ray-tracing quite time consuming. [35], [37]

4.2 LightTools: a ray-tracing tool

LightTools is a ray-tracing simulation tool, developed by Optical Research Associates, that is suited for the simulation of LSCs because of its possibilities to simulate the behavior

of luminescent materials accurately. Developing a model of a certain configuration can be done using the interactive interface or via command line. The program has both forward and backward ray-tracing possibilities, of which only the first was used. Outputs at different places can be registered using so called 'detectors'. Results can be viewed in table or graph and can be exported easily.

A picture of the model, as displayed by the program can be seen in figure 4.1. The source is modeled as a bar with the lower surface emitting light at some micrometers from the LSC. The spectrum of the light source is entered as measured in the previous chapter and the angular dependence is supposed to be lambertian.

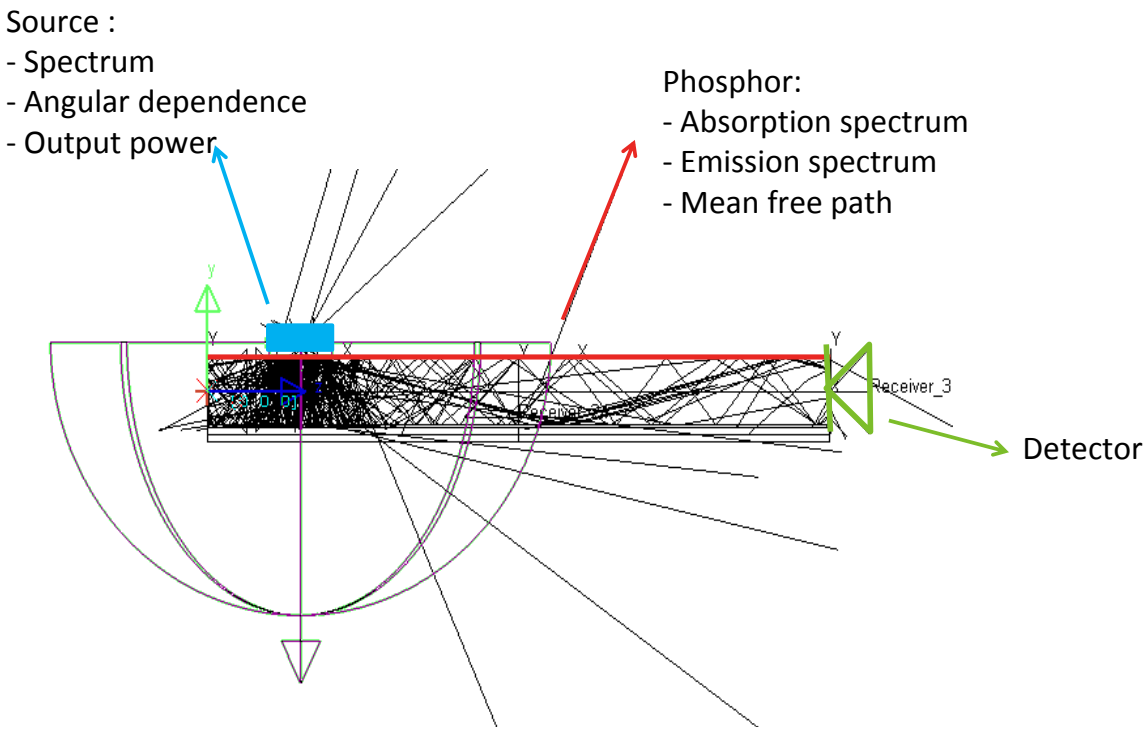

Figure 4.1: Model of the LSC in LightTools.

The concentrator itself is modeled as two plates in optical contact with each other. The upper plate is only a few micrometers thick and represents the coating. The lower plate represents the PMMA plate. The absorption spectrum and refractive index of the PMMA used in the experiments had been measured at TU/e before and are introduced using a user defined material.

To model the Luminescent material in the coating, the absorption and emission spectrum (without reabsorption)are needed, as well as the refractive index of the coating, which is taken to be equal to that of PMMA. The quantum yield of this dye is approximately 1 and is entered as one in the model. The angular dependence of the emission is set to be uniform. Earlier use of the program has indicated that setting the absorption to one for all wavelengths and including the absorption properties of the dye into the wavelength dependent mean free path leads to better results. The relation between the absorption and the mean free path is given in equation 4.1, with t_{layer} the thickness of the coating. The absorption spectrum should be measured for a sample with the same concentration,

by measuring it in transmission in a spectrometer, with perpendicular illumination, and the spectrum of a blank sample should be subtracted. Since in this measurement, the pathlength of the light through the coating is indead equal to its thickness, so no extra corrections for the angle of incidence has to be applied.

$$\begin{aligned} Transmission(\lambda) &= 1 - Absorption(\lambda) \\ &= \exp\left(-\frac{t_{layer}}{MFP(\lambda)}\right) \\ MFP(\lambda) &= -\frac{t_{layer}}{\ln(1 - Abs(\lambda))} \end{aligned} \tag{4.1}$$

4.3 Performed simulations

In this section a list will be made of which parameters led to which results. The discussion of the results and the comparison with the measurements will be done in the next section.

The calculation of the amount of light absorbed by the dye layer and the resulting collection efficiency is done in the same way as in chapter 3. The spectrum of the blue side emitting source (figure 3.5) is used, as well as the luminescent spectra from the simulations. The resolution of the simulation detector is set to 1 nm and the number of simulated rays was 1 000 000. However, this leads to rather noisy spectra as can be seen in the left graph of figure 4.2. To give a better idea of the shape of the spectra, a floating average over five measurment is taken which results in pictures as the one at the right in figure 4.2. For calculations the original spectra were used.

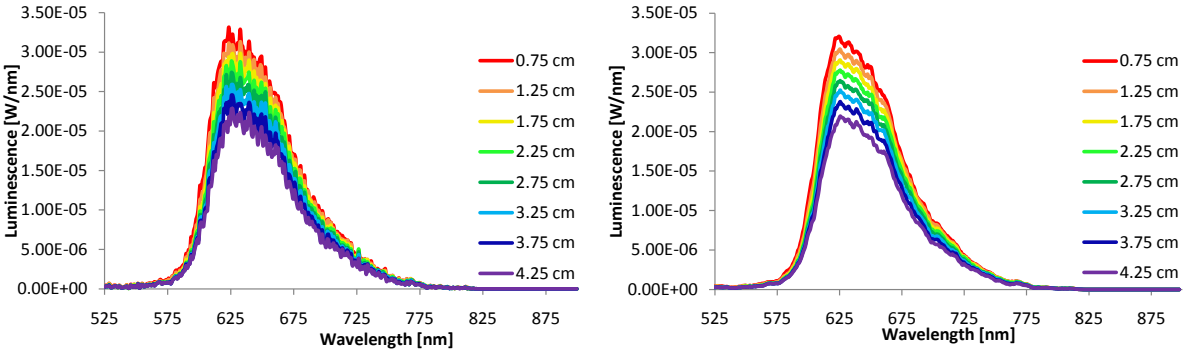

Figure 4.2: Example of simulated luminescence spectra as they come out of LightTools (left) and after taking a 5 point floating average (right).

4.3.1 Parameters

There were two properties of the LSC that we could not measure precisely to implement them in our model, but of which we do expect a certain influence on the results. The first one is related to the absorption spectrum of the dye, which we could only measure accurately up to 650 nm. Although the absorption probability at this wavelength is already below 0.02, it could still be important how far the tail of this absorption spectrum extends into the (infra)red. We will thus compare simulation results for which we used

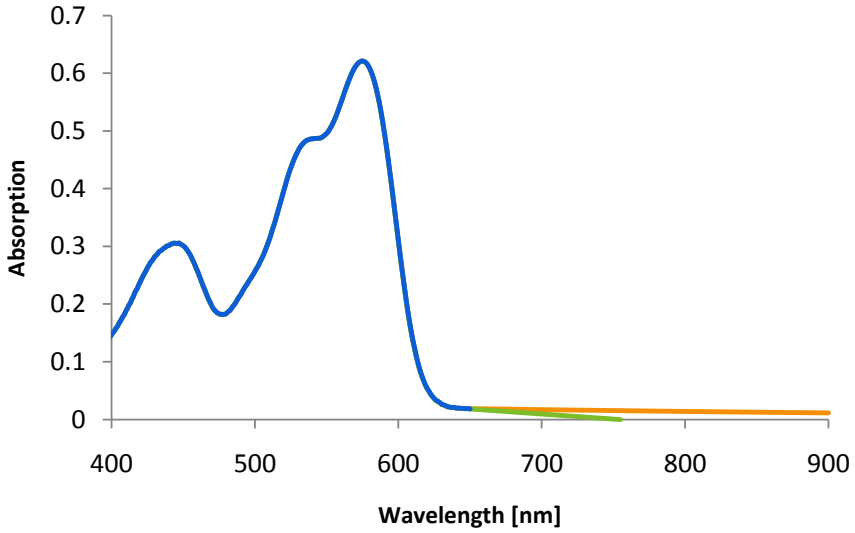

Figure 4.3: Measured absorption spectrum up to 650 nm and possible tails which were added to study the influence of the tail of the absorption spectrum on the luminescent output.

the absorption spectrum without fitted tail (blue curve in figure 4.3), with a short tail that goes to zero at about 750 nm (based on absorption measurement results described in [29], green curve in figure 4.3), and with a long tail (orange curve in figure 4.3).

Also the scattering properties of the edges of the waveguide plate were difficult to estimate. Although we suppose that part of the light is specularly reflected, and part of it is scattered, we did not know any quantities related to this reflection or scattering. Therefore they were taken as a parameter: the two extreme possibilities (100% Lambertian scattering and 100% specular reflection: LightTools option smooth optical) were simulated as well as some intermediate settings containing both scattering and reflection. The back edge was always taken to be absorbing because it had been painted black in the experimental situation. Although it was not expected to be physically relevant, one simulation with 3 completely absorbing edges and 1 Lambertian scattering edge was also performed.

The intermediate settings containing scattering and specular reflection are made possible by the complete scattering options of edges for all objects in LightTools. In this complete scattering module the portion of the light that is reflected and transmitted can be specified. For both the transmitted and the reflected light you can then chose how much of it should be reflected in a diffuse and how much in a near specular way. The near specular distribution function also can be specified by the user, for example Gaussian, cosine to the n^th power, etc.

In total 4 complete scattering combinations were simulated:

- Complete scattering 1: 50% transmitted of which 50% diffuse and 50% near specular (cos^5), and 50% reflected of which 50% diffuse and 50% near specular (cos^5).

Table 4.1: Overview of the performed simulations.

	100% absorbing	100% scattering	Smooth optical	Complete scattering 1	Complete scattering 2	Complete scattering 3	Complete scattering 4
Short tail	x	x	x	x	x	x	x
No tail		x	x				
Long tail		x	x				

- Complete scattering 2: 75% transmitted of which 50% diffuse and 50% near specular (cos^5), and 25% reflected of which 50% diffuse and 50% near specular (cos^5).
- Complete scattering 3: 25% transmitted of which 50% diffuse and 50% near specular (cos^5), and 75% reflected of which 50% diffuse and 50% near specular (cos^5).
- Complete scattering 4: 50% transmitted of which 50% diffuse and 50% near specular (cos^{50}), and 50% reflected of which 50% diffuse and 50% near specular (cos^{50}).

An overview of all performed simulations can be found in table 4.1. In the next subsections all simulation results are given. In section 4.4 the results will be compared and discussed more extensively.

4.3.2 No absorption tail, 100% scattering

In this simulation all edges are Lambertian scatterers with equal probability of scattering inwards and outwards. The absorption spectrum of the dye is used as measured, without any fitted tails abouve 650 nm. The resulting Watt to Watt collection efficiencies are quite high for excitation close to the measurement edge, but decrease rapidly due to reabsorption.

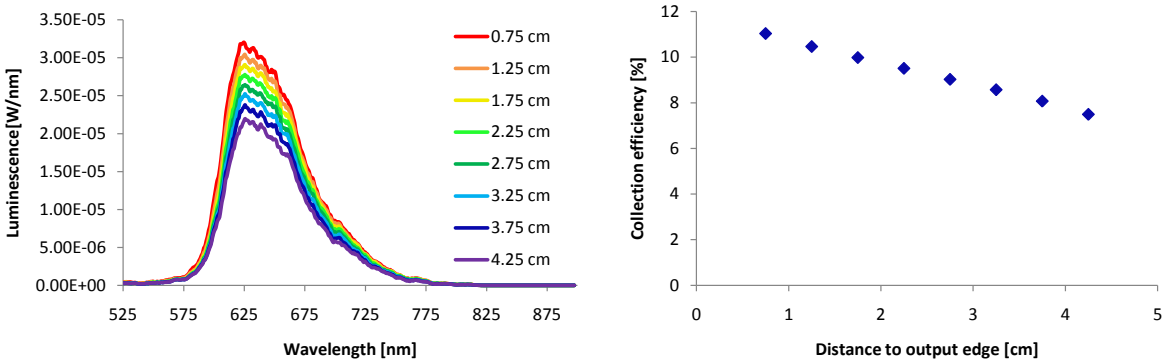

Figure 4.4: Resulting spectra (left) and Watt to Watt collection efficiencies (right) as a function of distance of excitation to the output edge for the simulations with no absorption tail and 100% scattering edges.

4.3.3 No absorption tail, smooth optical

In this simulation all edges are considered to be smooth optical interfaces, that yield only specular reflection and transmission. This means that most of the light is kept inside at the side edges, but also at the front edge the light now has more difficulties to couple out. The Watt to Watt collection efficiency as a function of excitation distance is almost constant with even an increase in the first half and a slight decreas in the second half of the LSC plate.

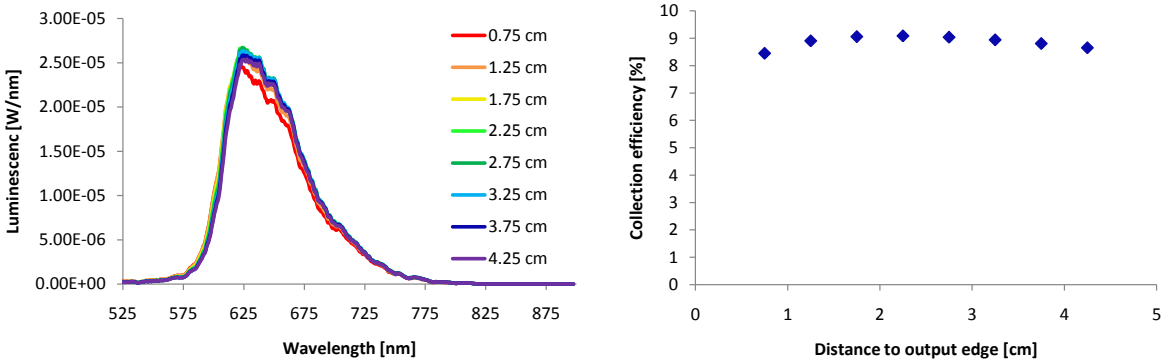

Figure 4.5: Resulting spectra (left) and Watt to Watt collection efficiencies (right) as a function of distance of excitation to the output edge for the simulations with no absorption tail and smooth optical edges.

4.3.4 Long absorption tail, 100% scattering

In this simulation the absorption spectrum with the long tail fitted to it is used, as well as 100% scattering interfaces. The collection efficiency decreases with the distance to the output edge.

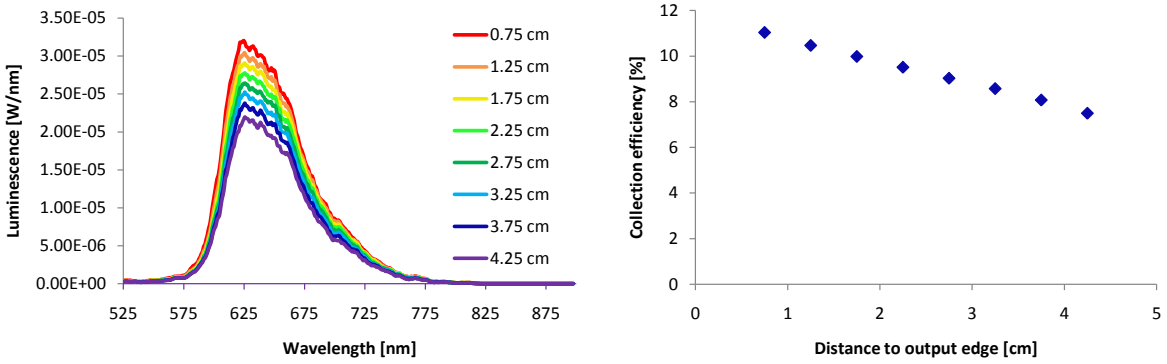

Figure 4.6: Resulting spectra (left) and Watt to Watt collection efficiencies (right) as a function of distance of excitation to the output edge for the simulations with a long absorption tail and 100% scattering edges.

4.3.5 Long absorption tail, smooth optical

The long absorption tail and the optically smooth edges were used for this simulation.

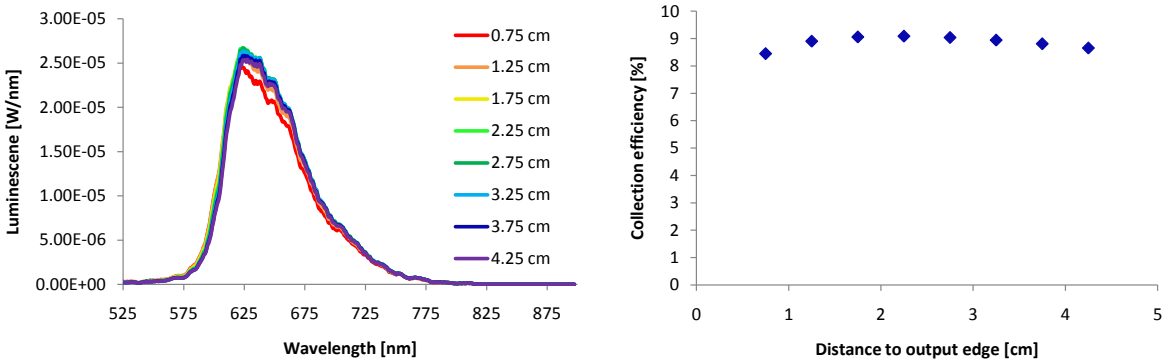

Figure 4.7: Resulting spectra (left) and Watt to Watt collection efficiencies (right) as a function of distance of excitation to the output edge for the simulations with a long absorption tail and smooth optical edges.

4.3.6 Short absorption tail, 100% scattering

In this simulation the absorption spectrum with the short, most realistic tail was used as well as 100% scattering edges.

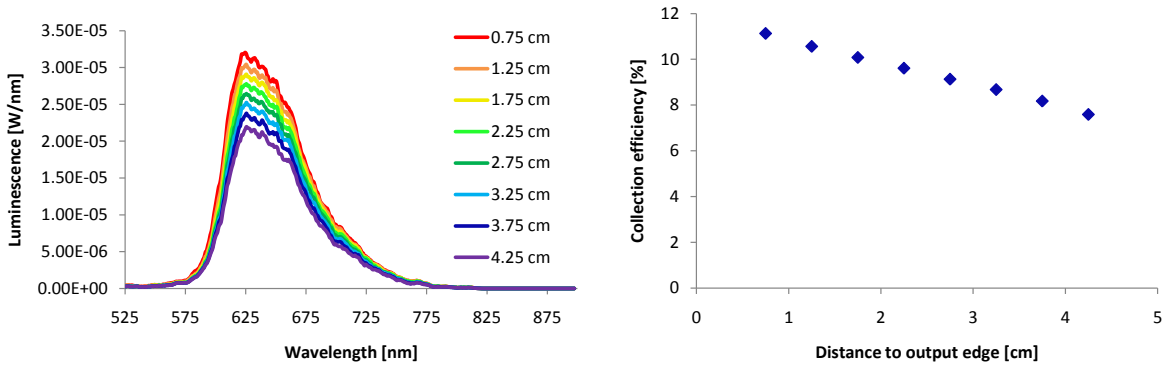

Figure 4.8: Resulting spectra (left) and Watt to Watt collection efficiencies (right) as a function of distance of excitation to the output edge for the simulations with a short absorption tail and 100% scattering edges.

4.3.7 Short absorption tail, smooth optical

Short absorption tail and smooth optical edges result in the spectra and collection efficiencies depicted in figure 4.9

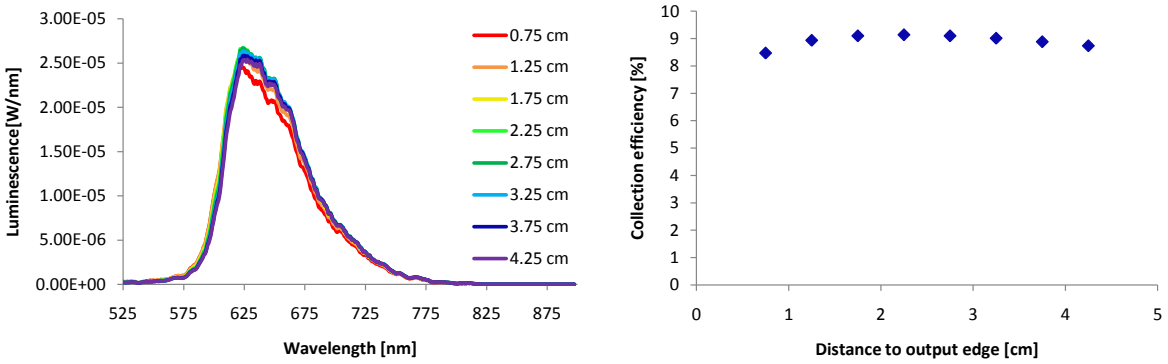

Figure 4.9: Resulting spectra (left) and Watt to Watt collection efficiencies (right) as a function of distance of excitation to the output edge for the simulations with a short absorption tail and smooth optical edges.

4.3.8 Short absorption tail, 100% absorbing

In this simulation, not only the back edge, but also the two side edges were supposed to be 100% absorbing, whereas the measurement edge was modelled to be lambertian scattering. This leads, as expected, to quite low Watt to Watt collection efficiencies, aspecially at larger distances.

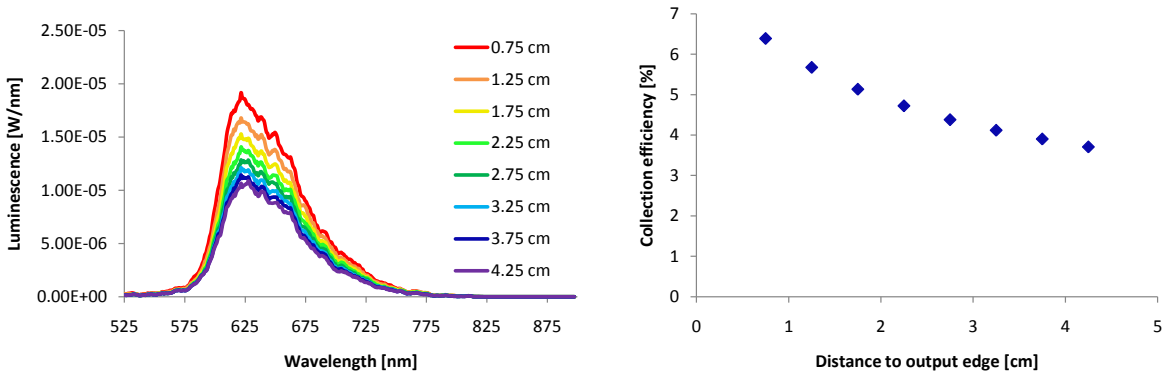

Figure 4.10: Resulting spectra (left) and Watt to Watt collection efficiencies (right) as a function of distance of excitation to the output edge for the simulations with a short absorption tail and 100% absorbing edges.

4.3.9 Short absorption tail, complete scattering 1

For the first complete scattering simulation, half of the light is reflected, and half of it transmitted, for both the reflected and the transmitted light one half is taken to be diffuse and the other half near specular. The near specular distribution is set to be cos^5.

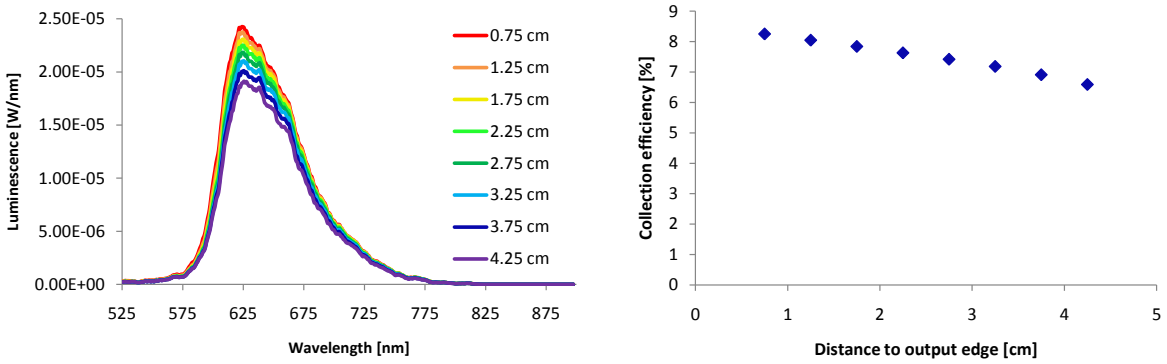

Figure 4.11: Resulting spectra (left) and Watt to Watt collection efficiencies (right) as a function of distance of excitation to the output edge for the simulations with a short absorption tail and edges modelled according to complete scattering 1.

4.3.10 Short absorption tail, complete scattering 2

For the second complete scattering simulation, 75% of the light is transmitted at each edge, and only 25% is reflected; Again half diffuse and half near specular with a cos^5 distribution. This will lead to more losses at the side edges, but also to better outcoupling at the measurement edge.

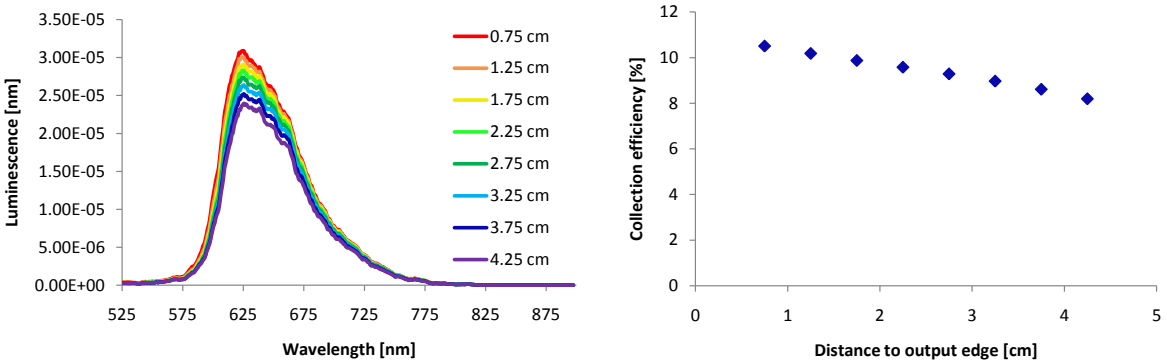

Figure 4.12: Resulting spectra (left) and Watt to Watt collection efficiencies (right) as a function of distance of excitation to the output edge for the simulations with a short absorption tail and edges modelled according to complete scattering 2.

4.3.11 Short absorption tail, complete scattering 3

The third complete scattering simulation is the opposite of the second. This time, most of the light (75%) is reflected, and only 25% is transmitted. The Ratios for diffuse and near specular stay the same, as well as the near specular distribution function.

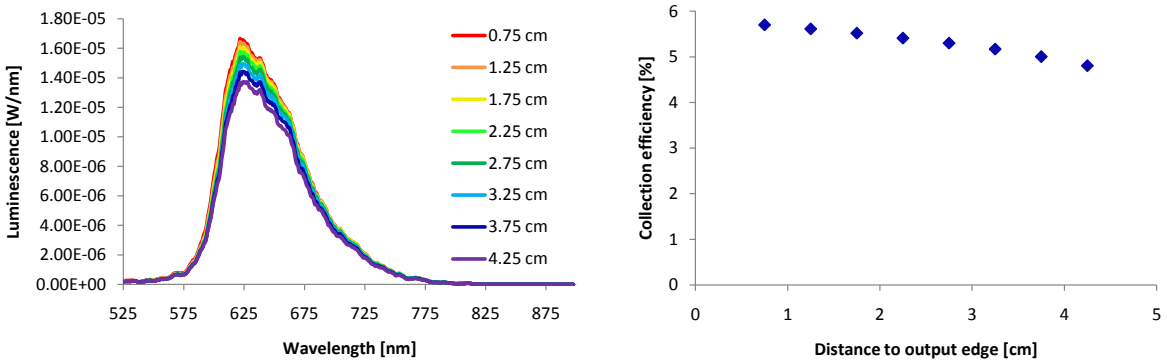

Figure 4.13: Resulting spectra (left) and Watt to Watt collection efficiencies (right) as a function of distance of excitation to the output edge for the simulations with a short absorption tail and edges modelled according to complete scattering 3.

4.3.12 Short absorption tail, complete scattering 4

With the last complete scattering simulation, we want to check wether it makes a difference if the near specular distribution is made even more narrow than it already is. Therefore, we use the same settings as for complete scattering 1, but with cos^{50} as a near specular distribution function.

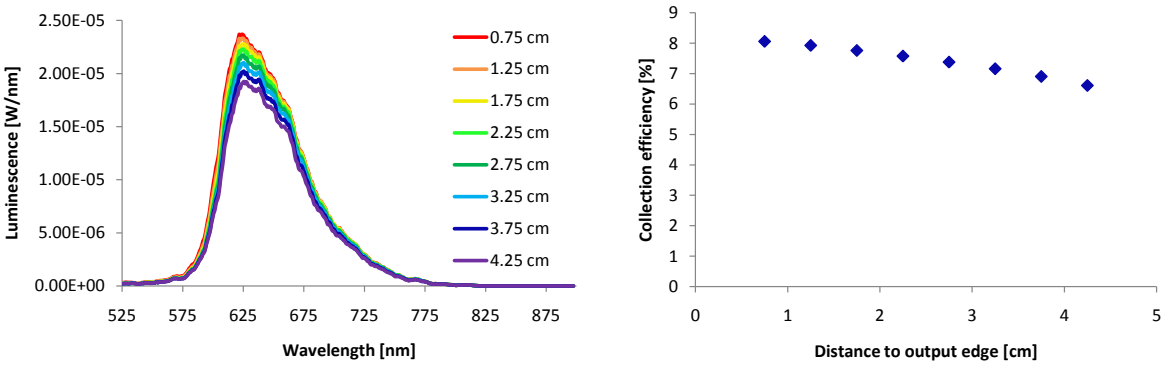

Figure 4.14: Resulting spectra (left) and Watt to Watt collection efficiencies (right) as a function of distance of excitation to the output edge for the simulations with a short absorption tail and edges modelled according to complete scattering 4.

4.4 Discussion of the results

4.4.1 Influence of the absorption tail

The influence of the absorption tail on the collection efficiency can be seen in figure 4.15. Let us concentrate on the simulations with the long (coinciding with the 'no tail' simulation points in the graph) and short absorption tails, because these are the most realistic (no discontinuity in absorption spectrum). We see a small difference in the collection efficiency of about 0.1%. If we look at the spectra in figure 4.16, we see that the spectra are also slightly shifted at the long wavelength edge.

Important to notice is that with the noisy spectra we are working with, these differences are probably not even significant and certainly very small. The small differences can be expected, because the low absorption values in the tail lead to long absorption lengths, and thus differences, can not be seen in small samples. It can be concluded that if similar situations, where an absorption tail that is already at a very low level can not be measured up to very high wavelengths, occur in the future, one should not worry about the consequences of this in simulation results at this resolution and with this sample size and this amount of rays.

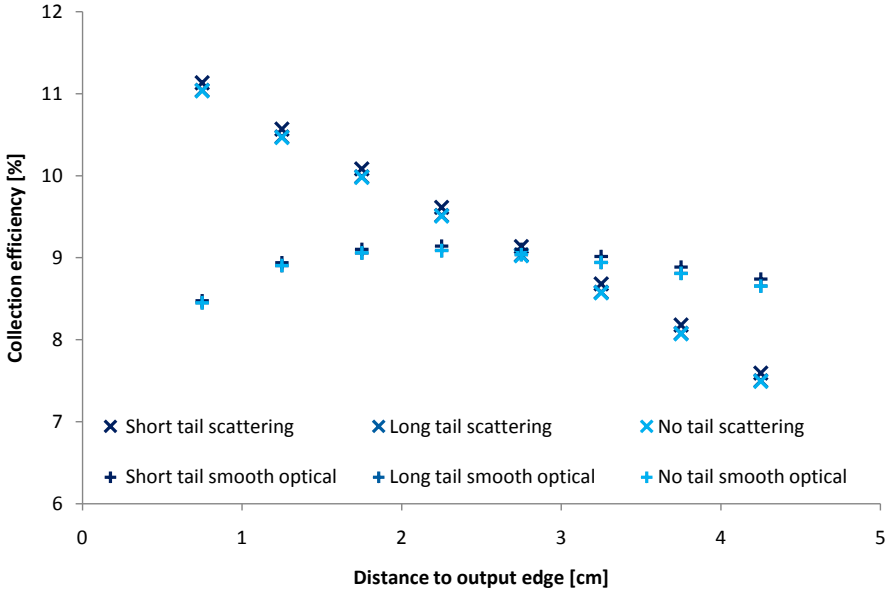

Figure 4.15: Simulated Watt to Watt collection efficiencies comparing the simulations with different absorption tail properties.

4.4.2 Influence of the properties of the sample edges

The properties of the sample edges have a much larger influence on the obtained result. This can be seen in figure 4.17, where the Watt to Watt collection efficiencies for the different simulations (all with the short tail absorption) and the experimental situation.

The collection efficiency of the smooth optical simulation shows the most remarkable dependency on the excitation distance. To understand this we must think of the outcoupling of light (which is not at all efficient due to the smooth output edge), and reabsorption as two competing mechanisms. Some light rays emitted by a dye molecule simply do not have the right angle to get out of the LSC plate unless after reabsorption and reemission in a more suitable direction. Increasing the distance to the output edge gives those rays more chances to be coupled out at this edge. However, reabsorption also yields loss, and at a certain distance this becomes more important. From this distance onwards, the path to the output edge is so far, that multiple reabsorptions strongly limit the chances of a light ray to get there. This leads to the dependency depicted in figure 4.17. Also clear is that this situation is not comparable with the experimental one.

For the simulation of the LSC with 3 absorbing edges, the collection efficiency is quite low from the beginning, but also shows a rather steep decrease with increasing distance.

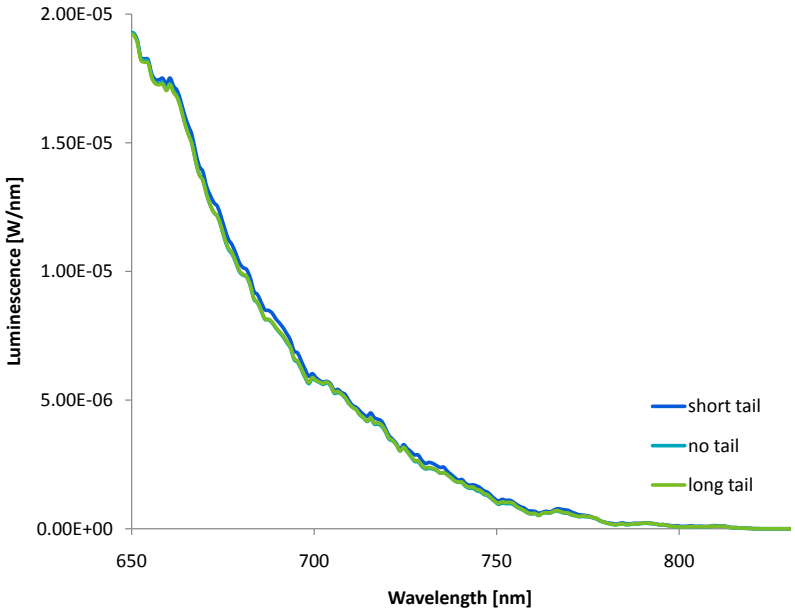

Figure 4.16: Detail of the long wavelength edge of the luminescent spectra obtained by simulation of the luminescent solar concentrator with scattering edges and excitation at 4.25 cm.

This is due to the fact that in this situation reflections at the side edges are not alowed. The further away from the output edge the sample is excited, the smaller the number of rays that can reach the edge without impinging on a side edge first. Also the solid angle with which a luminescent molecule sees the output edge, and thus the chance for a ray to reach it without any reflection gets smaller with increasing distance. It is clear that the decrease in collection efficiency is due to the edge absorption rather than to reabsorption, this is also the reason why the side edges were not painted black in the experiment.

If the edges of the sample are supposed to be lambertian scatterers, the collection efficiency is high close to the output edge, but also shows a steep decrease with increasing distance. This is because with increasing distance, the number of reflections increases, and every reflection yields a randomization of the propagation direction, which possibly leads to longer path lengths and thus smaller collection efficiencies. For short distances, the collection efficiencies are so high because the outcoupling is better than for example for smooth optical edges.

When looking at the result of the complete scattering simulations it can be noticed that there is no significant difference between complete scattering simulation 1 and 4. The directivity of the cos^5 near specular distribution is already sufficiently large, and increasing the power by a factot 10 does not make a big difference anymore.

Furthermore it can be noticed that increasing the amount of transmitted light leads to higher collection efficiencies. The improved outcoupling of light at the output edge is apparently more important than the increased losses at the edges. It is expected that there will be an optimal reflection transmission ration, where the two mechanisms are equally important. It certainly does not make sense to increase the transmission to 1 (if this would already be physically possible) because then you end up in a case similar

to the one with the 100% absorbing side edges. Optimal would be to have (alsmost) smooth optical side edges, and a scattering output edge which couples out as much light as possible. In practice extra mirrors and at the side edges and index matching and anti-reflection coatings at the output interface will improve the edge properties further.

The third complete scattering simulation is closest to the experimental situation. It uses edges that are 75% reflective and 25% transmissive, and a diffuse component of 50% . However, it would be premature to conclude that these are the real properties of the edges of the used samples. It is still desirable to perform specific measurements to determine the edge properties of the samples experimentally.

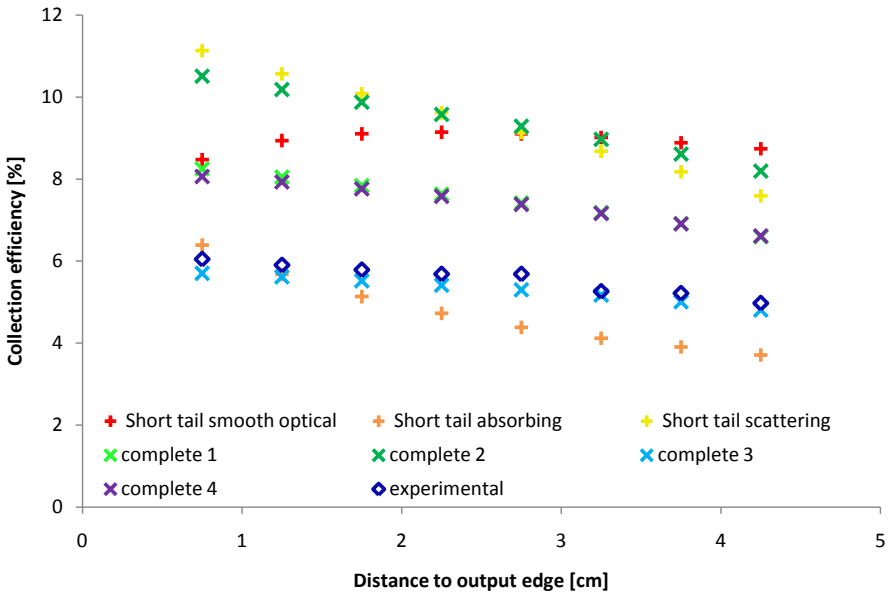

Figure 4.17: Overview of the Watt to Watt collection efficiencies of the simulations with different edge properties of the LSC-plate as well as the experimental collection efficiencies.

4.4.3 Comparison of the spectra with the measurements

The best way to see if the reabsorption is correctly modeled is not by looking at the collection efficiency, but by looking at the redshift of the spectra themselves or by calculating the reabsorption probability. To calculate the reabsorption probability you need a first time emission spectrum. There are two approaches here, one is to use the measured spectrum, but scaling the noisy simulated emission spectra to fit the tail of this measured spectrum could not be done in a consistent way. Also the second approach of trying to simulate the measurement with which the first time emission spectrum was obtained did not lead to any qualitative output.

The simulated and experimental spectra at 0.75 cm (closest) and 4.25 cm (furthest) are given in figure 4.18. Close to the measurement edge, simulation and experiment seem to be consistent. However, at a larger distance we see that the simulated spectrum has not shifted as much to the red as the experimental one. The Light Tools model we are using does not seem to be 100% correct in simulating the reabsorption processes taking place in the concentrator.

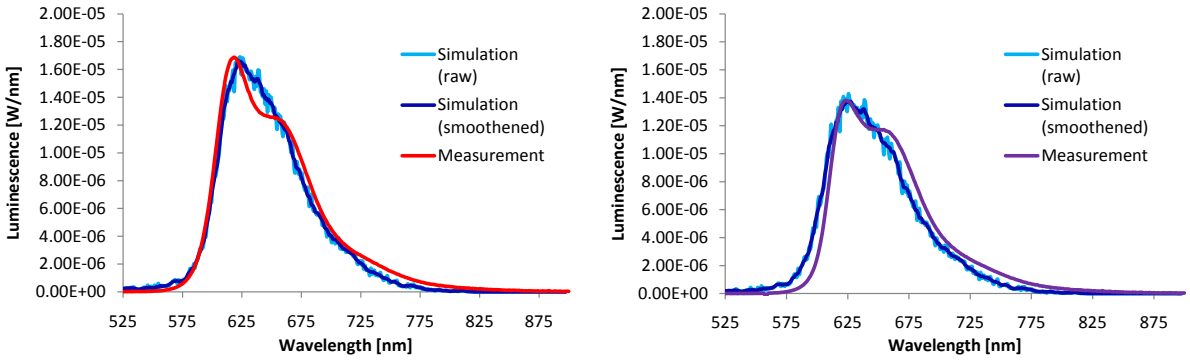

Figure 4.18: Comparison of the spectra obtained by the experiment and the simulation (complete scattering 3) for excitation at 0.75 cm (left) and 4.25 cm (right) from the measurement edge.

The role of the properties of the sample edges in the correct simulation of reabsorption is not unimportant. We already suggested in the previous section that the steep decrease of the collection efficiency as a function of excitation distance for the simulation with the 100% scattering edges could be caused by longer pathlengths due to randomization of the propagation direction at the edges. If we now take the spectrum of the simulation at 4.25 cm for the sample with 100% scattering edges, and scale it so that the area under it equals that of the comlete scattering 3 simulated spectrum at this excitation distance, we find a larger redshift and a better approximation of the measured spectrum (figure 4.19).

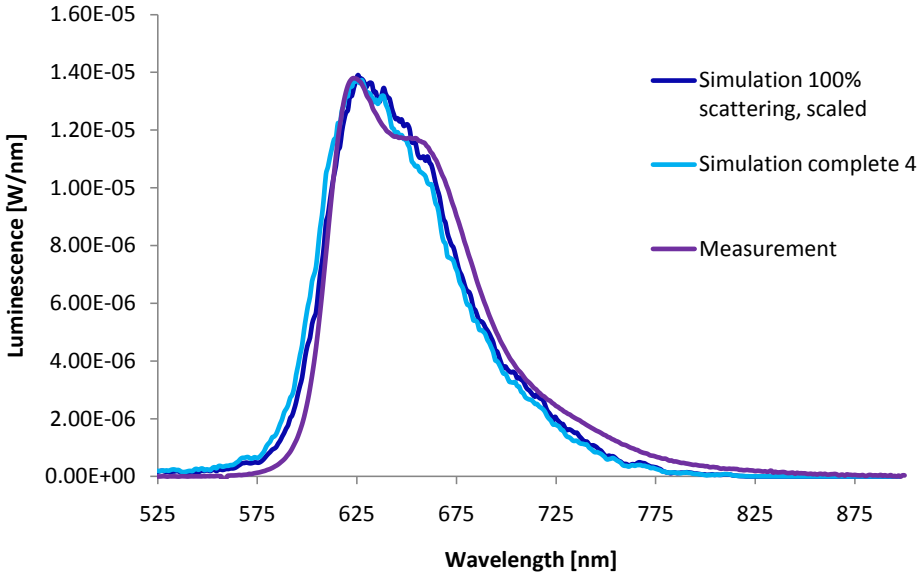

Figure 4.19: comparison of the measured and simulated spectra at 4.25 cm.

It can be concluded that a correct characterisation of the properties of the sample

edges is vital to the modelling of reabsorption in a luminescent solar concentrator. They determine the pahtlength of the light and thus also the number of reabsorption events. It is however expected that the influence of the edges will decrease with increasing sample size.

Chapter 5

Conclusion

The role of renewable resources on the energy market becomes more and more important. Solar energy is one of the options. just like the other renewables,it has a lot of advantages, but also some disadvantages that still have to be overcome. For solar energy in particular the high cost of silicon and other semiconductor materials used, and the fact that currently only a small part of the solar spectrum can efficiently be converted to electricity are the most important drawbacks.

Luminescent solar concentrators are proposed to solve at least one of the problems, and in addition create more design flexibility for integration in different kind of applications. By replacing the large and expensive semiconductor plate by a plastic plate doped with luminescent material and only putting small area photovoltaic cells at one or more edges the cost can significantly reduced. However, losses remain an important issue in LSCs.

In this thesis work experiments and computer simulations were used to get a better understanding of one particular and important loss mechanism: reabsorption losses. With that purpose, one particular dye, Lumogen F Rot (from BASF), that is often used in LSC research has been studied. An experimental set-up was build, in which the luminescent spectrum at one output edge of a 50x50x5 mm sample, locally illuminated with a narrow-band lightsource (an LED) could be measured. The ray tracing based simulation program LightTools was used to simulate the experimental situation and results of simulations and experiments were compared.

Two quantities were found usefull to characterize losses in LSCs in general and reabsorption losses in particular. The first one is the collection efficiency, which characterizes the losses from the moment that a photon is absorbed by the dye molecule until the outcoupling of the light at the measurement edge. Together with the absorption efficiency and the photovoltaic cell external efficiency this collection efficiency will determine the overall efficiency of the luminescent solar concentrating system. The collection efficiency can be expressed in terms of energy or photon flux, both definitions were used in this text.

Another characteristic quantity is more specificly related to reabsorption losses. It is called the reabsorption probability (P_r) and it expresses the probabiltiy that a luminescent photon, that was emitted for the first time by a luminescent molecule after excitation by the source, can reach the output edge without suffering reabsorption. Often also $1 - P_r$, called the survival probability is used.

Both the collection efficiency and the reabsorption probability were calculated out of spectra measured for excitation of the 50x50x5 mm sample by a blue and green LED source of 50x5 mm at different distances from the measurement edge. As expected the results for both sources coincided, and both the collection efficiency and the survival probability showed a decrease with increasing distance of the excitation to the output edge.

For the simulation of the experimental set-up there were problems in het definition of the model because the exact properties of the sample edges were unknown. Also the tail of the absorption spectrum of the dye could not be measured, but fitting different tails to the measured spectrum did not lead to much difference in the obtained results, so this was not a problem. Different sample edge properties on the other hand (lambertian scattering, specular reflecting etc.) dit lead to large differences in both the obtained output spectra and the calculated collection efficencies. Without knowledge of the edge properties of the sample it is impossible to establish a correct model for raytracing

Despite the many problems encountered, I do think that this method could be usefull for reabsorption characterisation and comparison of different dyes and for checking the working of the raytracing model and if necessary finetuning it before using it for further simulation of larger systems and possible prototypes. I will list up some steps that, in my opinon will have to be taken to make this method more usefull and reliable.

Experiment: comparing reabsorption properties of different dyes, differently alligned dyes etc.

The set-up that was used in this thesis work and is displayed in 3.3 can be further used to characterise the reabsorption probabilities of different dyes. The LED source used must be chosen to match the high absorption wavelengths of the dye, but not to overlap the emission spectrum of it. The back edge of the sample will have to be painted black. The output spectra at the front edge will be measured. Also a first time emission spectrum has to be measured in order to calculate the reabsorption probability. The collection efficiency and the survival probability can be plotted as function of the excitation distance. The aim should be to develop a dye that has a high collection efficiency, and for which the collection efficiency and survival probability do not decrease too much with increasing excitation distance.

- Especially when dyes with better reabsorption characteristics (less overlap between absorption and emission spectrum) will be measured, it might be usefull to work with longer samples. The set-up can easily be adapted to samples with the same width but that are for example 10 cm long instead of 5.

- At all times one should keep an eye on LED stability and degradation. If new LED sources are constructed, good connections and a stable structure to keep everything in place should be implemented.

- The set up used is not ideal for measuring small signals. Especially for measuring the first time emission this leads to long measurement times and noisy signals. It would be good to look at solutions for this, either in the form of a stronger excitation source of a more sensitive detector.

- Until now the source has been placed manually onto the sample, and the shielding to prevent straylight from the source to enter the sample was rather primitive. Building a well encapsulated lightsource, that can be helt in position and moved to the right position with a translation stage would be a good idea if lots of measurements are going to be taken.

Simulation: controlling wether or not the simulation model correctly incorporates reabsorption

Before simulating systems under illumination of the complete solar spectrum, increasing the size of the simulated concentrator, simulating entire systems including mirrors, filters etc. simulating the experimental situation described before can give more information about the correctness of the reabsorption properties in the ray tracing model. Especially by comparing the spectra and collection efficiencies for excitation at different distances from the measurement edge from simulation and experiment will give a good indication of the correct implementation of reabsorption in the model.

- The most important task to make this work is the characterisation of the sample edge properties. a triangular sample with two polisched edges could be illuminated with a laser from one polished edge and a detector could detect the amount of specularly reflected light through an aperture at the other polished edge. A sample with tree polished edges could be used as a reference. Alternatively, manipulating the edge properties could lead to good results. I especially expect a sample with a lambertian scattering front edge and polished side edges to be usefull and easily implementable into the model.

- If the implementation of the reabsorption is not perfect even after introducing the correct edge parameters one can try to introduce a slightly higher or lower reabsorption by adjusting the mean free path or layer thickness in the model.

Bibliography

[1] A. Luque, A. Marti, A. Bett, V. M. Andreev, C. Jausaud, J. A. M. van Roosmalen, J. Alonso, A. Rauber, G. Strobl, and W. Stolz, "Fullspectrum: a new pv wave making more efficient use of the solar spectrum," *Solar Energy Materials and Solar Cells*, vol. 87, pp. 467–479, 2005.

[2] G. Smestad, *Optoelectronics of solar cells*. SPIE, The International Society for Optical Engineering, 2002.

[3] U. Rau, F. Einsele, and G. C. Glaeser, "Efficiencylimits of photovoltaic fluorescent collectors," *Applied physics letters*, vol. 87, p. 171101, 2005.

[4] G. Smestad, H. Ries, R. Winston, and E. Yablonovich, "The thermodynamic limits of light concentrators," *Solar Energy Materials*, vol. 21, pp. 99–111, 1990.

[5] A. M. Hermann, "Luminescent solar concentrators - a review," *Solar Energy*, vol. 29, pp. 323–329, 1982.

[6] W. H. Weber and J. Lambe, "Luminescent greenhouse collector for solar radiation," *Applied Optics*, vol. 15, pp. 2299–2300, 1976.

[7] A. A. Earp, G. B. Smith, J. Franklin, and P. Swift, "Optimisation of a three-colour luminescent solar concentrator daylighting system," *Solar Energy Materials and Solar Cells*, vol. 84, pp. 411–426, 2004.

[8] P. Swift and G. B. Smith, "Color considerations in fluorescent solar concentrator stacks," *Applied Optics*, vol. 42, pp. 5112–5117, 2003.

[9] T. Markvart, "The thermodynamics of optical etendue," *Journal of Optics A: pure and applied optics*, vol. 10, 2008.

[10] P. Scudo, L. Abbondanza, and R. Fusco, "Spectral converters and luminescent solar concentrators," *arXiv preprint*, vol. 0907.3551, 2009.

[11] D. K. G. de Boer, "Optimizing wavelength-selective filters for luminescent solar concentrators," *SPIE proc.*, vol. 7725, april 2010.

[12] A. Zastrow, "The physics and applications of fluorescent solar concentrators: a review," *SPIE*, vol. 2255, pp. 534–547, 1994.

[13] B. Rowan, L. R. Wilson, and B. S. Richards, "Advanced material concepts for luminescent solar concentrators," *IEEE journal of selected topics in quantum electronics*, vol. 14, pp. 1312–1322, 2008.

[14] V. Sholin, J. D. Olson, and S. A. Carter, "Semiconducting polymers and quantum dots in luminescent solar concentrators for solar energy harvesting," *Journal of Applied Physics*, vol. 101, 2007.

[15] R. Reisfeld, "Future technological applications of rare-earth-doped materials," *Journal of the Less-Common Metals*, vol. 93, pp. 243–251, 1983.

[16] A. Goetzberger, *High-Efficient Low-Cost Photovoltaics*, vol. 140 of *Springer Series in Optical Sciences*, ch. 10, Fluorescent solar energy concentrators: principle and present state of development, pp. 159–176. Springer Berlin Heidelberg, 2009.

[17] J. C. Goldschmidt, M. Peters, F. Dimroth, A. W. Bett, L. Steidl, R. Zentel, M. Hermle, S. W. Glunz, and G. Willeke, "Developing large and efficient fluorescent concentrator systems." Presented at the 24th European PV solar energy conference and exhibition, september 2009.

[18] M. J. Currie, J. K. Mapel, T. D. Heidelm, S. Goffri, and M. A. Baldo, "High-efficiency organic solar concentrators for photovoltaics," *Science*, vol. 321, pp. 226–228, 2008.

[19] J. C. Goldschmidt, M. Peters, A. Bosch, H. Helmers, F. Dimroth, S. W. Glunz, and G. Willeke, "Increasing the efficiency of fluorescent concentrator systems," *Solar Energy Materials and Solar Cells*, vol. 93, pp. 176–182, 2009.

[20] J. C. Goldschmidt, M. Peters, L. Pronneke, L. Steidl, R. Zentel, B. Blasi, A. Gombert, S. Glunz, G. Willeke, and U. Rau, "Theoretical and experimental analysis of photonic structures for fluorescent concentrators with increased efficiencies," *Phys. Stat. Sol.*, vol. 205, pp. 2811–2821, 2008.

[21] M. G. Debije, M. Van, P. P. C. Verbunt, M. J. Kastelijn, R. H. L. van der Blom, D. J. Broer, and C. W. M. Bastiaansen, "Effect on the output of a luminescent solar concentrator on application of organic wavelength-selective mirrors," *Applied Optics*, vol. 49, pp. 745–751, 2010.

[22] C. L. Mulder, P. D. Reusswig, A. M. Velazquez, H. Kim, C. Rotschild, and M. A. Baldo, "Dye alignment in luminescent solar concentrators: 1. vertical alignment for improved waveguide coupling," *Optics Express*, vol. 18, pp. 79–90, 2010.

[23] P. P. C. Verbunt, A. Kaiser, K. Hermans, C. W. M. Bastiaansen, D. J. Broer, and M. G. Debije, "Controlling light emission in luminescent solar concentrators through use of dye molecules aligned in a planar manner by liquid crystals," *Advanced Functional Materials*, vol. 19, pp. 2714–2719, 2009.

[24] A. De Vos and F. Strubbe, "Solar cells, notes accompanying course 900132: photovoltaic solar energy conversion.." Ghent University.

[25] Y.-H. Zhang, "Research highlights of the optoelectronics group at arizona state university." on-line: `http://asumbe.eas.asu.edu/`.

[26] W. G. J. H. M. van Sark, "Teaching the relation between solar cell efficiency and annual energy yiels," *European journal of physics*, vol. 28, pp. 415–427, 2007.

[27] D. Feuermann and J. M. Gordon, "High-concentration photovoltaic designs based on miniature parabolic dishes," *Solar Energy*, vol. 70, pp. 423–430, 2001.

[28] BASF, "Lumogen f rot 305, product specification." on-line: http://www.performancechemicals.basf.com/ev-wcms-in/internet/de_DE/function/evproducts:/document/30133188/TDS.

[29] L. R. Wilson, B. Rowan, N. Robertson, O. Moudam, A. C. Jones, and B. S. Richards, "Characterization and reduction of reabsorption losses in luminescent solar concentrators," *Applied Optics*, vol. 49, pp. 1651–1661, 2010.

[30] C. Ronda, *Luminescence: from theory to applications*, ch. 1: Emission and excitation mechanisms of phosphors, pp. 1–34. Wiley-VCH, 2008.

[31] Oceanoptics, "Usb optical bench options." on-line: http://www.oceanoptics.com/product/benchoptions_usb4.asp.

[32] Sony, "Sony ilx 511, 2048 pixel ccd linear image sensor (b/w): Datasheet." on-line: http://www.oceanoptics.com/technical/detectorsonyILX511.pdf.

[33] P. Kittidachachan, L. Danos, T. Meyer, N. Alderman, and T. Markvart, "Photon collection efficiency of fluorescent solar collectors," *Chimia*, vol. 61, no. 12, pp. 780–786, 2007.

[34] T. Dienel, C. Bauer, I. Dolamic, and Brühwiler, "Spectral-based analysis of thin film luminescent solar concentrators," *Solar Energy*, vol. 84, pp. 1366–1369, 2010.

[35] C. K. Lo, Y. S. Lim, S. G. Tan, and F. A. Rahman, "A new hybrid algorithm using thermodynamic and bacward ray-tracing approaches for modeling luminescent solar concentrators," *Energies*, vol. 3, pp. 1831–1860, 2010.

[36] A. J. Chatten, D. Farell, C. Jermyn, P. Thomas, B. F. Buxton, A. Büchtemann, R. Danz, and K. W. J. Barnham, "Thermodynamic modeling of luminescent solar concentrators," *IEEE*, pp. 82–85, 2005.

[37] A. R. Burgers, L. H. Slooff, R. Kinderman, and J. A. M. van Roosmalen, "Modelling of luminescent concentrators by ray-tracing," in *20th European photovoltaic solar energy conference and Exhibition*, 2005.